Development 114, 1003-1024 (1992)
Printed in Great Britain © The Company of Biologists Limited 1992

Altered mitotic domains reveal fate map changes in *Drosophila* embryos mutant for zygotic dorsoventral patterning genes

KAVITA ARORA* and CHRISTIANE NÜSSLEIN-VOLHARD

Max-Planck Institut fur Entwicklungsbiologie, Spemannstrasse 35/III, D7400, Tübingen, Germany

*Present address: Department of Molecular Biology and Biochemistry, University of California, Irvine, CA92717, USA

Summary

The spatial and temporal pattern of mitoses during the fourteenth nuclear cycle in a *Drosophila* embryo reflects differences in cell identities. We have analysed the domains of mitotic division in zygotic mutants that exhibit defects in larval cuticular pattern along the dorsoventral axis. This is a powerful means of fate mapping mutant embryos, as the altered position of mitotic domains in the dorsoventral pattern mutants correlate with their late cuticular phenotypes.

In the mutants *twist* and *snail*, which fail to differentiate the ventrally derived mesoderm, mitoses specific to the mesoderm are absent. The lateral mesectodermal domain shows a partial ventral shift in *twist* mutants but a proportion of ventral cells do not behave characteristically, suggesting that *twist* has a positive role in the establishment of the mesoderm. In contrast, *snail* is required to repress mesectodermal fates in cells of the presumptive mesoderm. In the absence of both genes, the mesodermal and the mesectodermal anlage are deleted.

Mutations at five loci delete specific pattern elements in the dorsal half of the embryo and cause partial ventralization. Mutations in the genes *zerknüllt* and *shrew* affect cell division only in the dorsalmost cells corresponding to the amnioserosa, while the genes *tolloid*, *screw* and *decapentaplegic* (*dpp*) affect divisions in both the prospective amnioserosa and the dorsal epidermis. We demonstrate that in each of these mutants dorsally placed mitotic domains are absent and this effect is correlated with an expansion and dorsal shift in the position of more ventral domains. The loss of activity in each of the five genes results in qualitatively similar alterations in the mitotic pattern; mutations with stronger ventralizing phenotypes affect increasingly greater subsets of the dorsal cells. Double mutant analysis indicates that these genes act in a concerted manner to specify dorsal fates. The correlation between phenotypic strength and the progressive loss of dorsal pattern elements in the ventralized mutants, suggests that one of these gene products, perhaps *dpp*, may provide positional information in a graded manner.

Key words: *Drosophila* embryogenesis, developmental genetics, pattern formation.

Introduction

The establishment of pattern along the two major body axes of the *Drosophila* embryo depends on the coordinated activity of a set of maternal and zygotically expressed genes (reviewed in Ingham, 1988). The various maternal genes that define the dorsoventral (DV) axis are integrated into a single system of positional information (Anderson et al., 1985 a, b; reviewed in Anderson, 1987; Nüsslein-Volhard and Roth, 1989; Rushlow and Arora, 1990). The normal function of these genes results in the establishment of a nuclear gradient of the *dorsal* (*dl*) protein (Steward et al., 1988). In the syncitial blastoderm embryo, nuclei on the ventral side contain the highest levels of *dl*, while the protein is excluded from nuclei in dorsal positions (Roth et al., 1989; Steward, 1989; Rushlow et al., 1989). The product of the *dl* gene is structurally homologous to the mammalian transcription factor NF-κB and the avian *rel* oncogene (Steward, 1987; Ghosh et al., 1990; Kieran et al., 1990).

dl protein has been shown to bind *cis*-regulatory sequences of downstream zygotic genes and is expected to function directly as a transcriptional regulator (Ip et al., 1991; Thisse et al., 1991). The *dl* gradient appears to regulate positional information in the embryo by activating the zygotic genes *twist* (*twi*) and *snail* (*sna*) in ventral cells and restricting *zen* and *dpp* expression to dorsal cells of the blastoderm (Thisse et al., 1987; Rushlow et al., 1987a; Roth et al. 1989; Steward, 1989; Ray et al., 1991). The *twi* and the *sna* transcripts are expressed in a single continuous stripe comprising the ventral 20% of the embryo (Thisse et al., 1987; Leptin and Grunewald, 1990; Ray et al., 1991), while the *zen* and *dpp* transcripts are expressed in a dorsal on-ventral off pattern, encompassing about 40% of the cells at

blastoderm (Rushlow et al., 1987b; St. Johnston and Gelbart, 1987). The initial patterns of RNA expression of *twi*, *sna*, *zen* and *dpp* are regulated entirely by maternal genes and are not altered by mutations in any of the known zygotic genes (Rushlow and Levine, 1990; Roth et al., 1989; Ray et al., 1991). These results suggest that *twi*, *sna*, *zen* and *dpp* are direct targets of *dl* and their regulation may represent the earliest subdivision of the DV axis into discrete regions of zygotic gene expression.

Zygotic genes involved in DV patterning characteristically exhibit a more limited effect on the pattern than maternal genes. This is substantiated by the observation that zygotic mutant phenotypes are comparable to those of weak maternal effect mutations that only partially dorsalize or ventralize the embryo. Complete loss-of-function mutations in maternal effect genes affect cell fates in the entire axis, so that in a dorsalized embryo all cells along the DV axis differentiate like dorsal cells in a normal embryo. Similarly, in extreme cases of ventralization, embryos consist only of ventral mesodermal derivatives (Nüsslein-Volhard, 1979; Anderson et al., 1985a; Anderson and Nüsslein-Volhard, 1986; Roth et al., 1991). In contrast, mutations in the zygotic genes *twi* and *sna* affect only a subset of the ventral pattern (Simpson, 1983; Grau et al., 1984; Nüsslein-Volhard et al., 1984), while mutations in the genes *zen* and *dpp* result in the restricted loss of dorsal pattern elements (Spencer et al., 1982; Nüsslein-Volhard et al., 1984; Wakimoto et al., 1984; Irish and Gelbart, 1987).

The zygotic genes *twi*, *sna* and *zen* encode proteins which show homology to characterized DNA-binding motifs (Rushlow et al., 1987b; Thisse et al., 1988; Murre et al., 1989; Boulay et al., 1987) and probably specify position information along the DV axis in a spatially restricted manner by regulating the transcription of other genes involved in the developmental pathway. On the other hand *dpp*, a member of the TGF-β superfamily of growth factors, is expected to influence development by means of cell communication pathways (Padgett et al., 1987).

Little is known about how other zygotic genes act to specify pattern along the DV axis. We present evidence that normal activity at three additional loci, *shrew* (*srw*), *screw* (*scw*) and *tolloid* (*tld*), is required early in development for the proper differentiation of dorsal pattern elements (Jürgens et al., 1984; this work). Mutations in all three genes result in ventralizing phenotypes like that of *zen* and *dpp* mutants; however, the degree of ventralization caused by mutants at individual loci varies. In this report we refer to these five genes collectively, as the decapentaplegic group genes.

Each of the dpp group mutants, as well as *twi* and *sna* mutants, show defects in development that are detectable at the begining of gastrulation and are indicative of alterations in cell fates. Cuticular markers are not sufficient to characterize and distinguish between the different mutant phenotypes. We have therefore examined the pattern of mitoses during cell cycle 14 (Foe and Alberts, 1983; Hartenstein and Campos-Ortega, 1985; Foe, 1989), to determine the fates of cells along the DV axis and map the regions of the embryo affected by mutations in the above genes.

We demonstrate that the altered cuticular pattern observed later in development reflects the altered mitotic behaviour of cells in discrete regions of the mutant embryo. We use the RNA expression pattern of the *single minded* (*sim*) gene (Thomas et al., 1988), which correlates with a specific mitotic domain, to demonstrate that the alteration of mitotic domains in the zygotic DV mutants closely reflects the altered transcription pattern of molecular markers in these mutants.

The analysis of a series of double mutants among this group of zygotic genes shows that genes required for dorsal pattern act independently of those required for ventral pattern. More than one zygotic gene appears to be responsible for the proper specification of a particular domain/region. On the ventral side, both *twi* and *sna* are required for normal development of the mesoderm and the mesectoderm. However, they show qualitatively different effects on the specification of the ventral region. In the absence of both gene products, ventral pattern elements are deleted and a subset of the mid-ventral cells do not behave normally. In contrast, in the dorsal half of the embryo, mutations in the genes *zen*, *srw*, *tld*, *scw* and *dpp* cause coordinated fate map shifts, in which the deleted pattern is compensated for by an expansion of ventrolateral pattern elements. This difference may reflect the distinct mechanism of pattern specification in the two regions. *twi* and *sna* both encode transcription factors and have comparatively independent and restricted effects on ventral pattern. The similarity in the phenotype of mutations affecting dorsal pattern, on the other hand, suggests that the ventralizing genes act in a concerted manner to specify dorsal fates. The nature of the phenotypic series encountered in the mutants of the dpp group suggests a dose-dependent response to some component of this pattern-forming process. We discuss our results in light of the fact that the *dpp* gene encodes a TGF-β homolog and may function as a secreted signal specifying dorsal development.

Materials and methods

Drosophila *strains*

The alleles of the various mutant genotypes used in this analysis are listed in Table 1. Null alleles of *twi* and *sna* used in this analysis were twi^{ID}, *Df(2R)twiS60* and sna^{IIG}. The wild-type stock was Oregon R. Flies were cultured on standard *Drosophila* cornmeal medium (Wieschaus and Nüsslein-Volhard, 1986). Crosses were reared at 25°C.

The genes *srw*, *scw* and *tld* were identified in screens for embryonic lethal mutations affecting the pattern of the larval cuticle (Nüsslein-Volhard et al., 1984; Jürgens et al., 1984). Only a single allele of the gene *scw*, called *l(2)IG76*, now named scw^{IG}, was isolated in this screen. The remaining alleles analysed in this study were recovered in a subsequent screen by U. Mayer, R. Lehmann and C. Nüsslein-Volhard

Table 1. *Matrix showing the relative phenotypic strength of ventralizing mutant alleles of the dpp group genes*

Locus-Map position	Deficiency	Allelic strength I	II	III	IV	V
zerknüllt (zen) 3-47.5	*Df(3R)LIN*	*f16**	*w36***			
shrew (srw) 3-15.0	*Df(3L)e13*	*10K*	*B18***			
screw (scw) 2-53.0	*Df(2L)TW9*	*O5* *IG*	*N5*	*C13*	*S12*** *E43*	
tolloid (tld) 3-85.0	*Df(3R)XTA1*	*5H* *7M*	*6B* *7O* *9D** *9K*	*7H* *8L* *9Q7* *9B*	*6P1* *6P4* *9Q1* *10E* *10F*** *B4***	
decapentaplegic (dpp) 2-4.0	*Df(2L)DTD2*	*r4*	*r4/r27*	*r27*	*r27/r92*	*Hin46***

Map position refers to genetic map position.

Class I and II, weakly ventralized; classes III and IV, moderately ventralized; class V, strongly ventralized phenotypes. For further classification, see Materials and methods.

*Temperature-sensitive alleles scored at 29°C.

**Alleles behave as apparent nulls at the respective loci.

(unpublished data). scw^{E43} was an embryonic lethal line identified by T. Wright, synonym *l(2)37Ff*. In the above screens, the mutagen used was ethyl methane sulphonate. The *Df(3L)e13*, srw^{B18} and tld^{B4} were recovered in screens carried out by E. L. Ferguson and K. V. Anderson. *zen* alleles are described by Wakimoto et al. (1984) and Rushlow et al. (1987). The alleles $dpp^{hin\text{-}r4}$, $dpp^{hin\text{-}r27}$, $dpp^{hin\text{-}r92}$, the haploinsufficient null allele dpp^{Hin46} and the deficiency *Df (2L) DTD2*, used in this study were obtained from W. M. Gelbart (Irish and Gelbart, 1987).

Analysis of embryonic phenotypes

Cuticle preparations were made from differentiated embryos, which were dechorionated, hand peeled out of their vitelline membranes with a fine needle, then fixed and embedded in a 1:1 mixture of Hoyers medium and lactic acid (Wieschaus and Nüsslein-Volhard, 1986).

The following criteria were used to distinguish class I to class V alleles, in addition to the general morphology and width of ventral denticle bands as described in the text for weak, moderate and strongly ventralized phenotypes. Class I: reduced amnioserosa, >50% mutants do not differentiate a ventral plate (pharyngeal skeleton) and distinct maxillary sense organs, 30% show a tail-up phenotype, Filzkörper morphology normal. Class II: >90% mutants lack amnioserosa, only ~20% differentiate maxillary sense organs, 50% lack antennal sense organs, Filzkörper morphology affected. Class III mutants show at least 20% increase in the width of denticle belts. Maxillary sense organs are missing and Filzkörper material is reduced in ~80% mutants. Class IV mutants show up to 35% increase in width of denticle belts. Less than 30% differentiate antennal sense organs, >50% show severe reduction of Filzkörper material. Class V mutants show complete rings of ventral denticle around the entire width of the embryo. Pharyngeal skeletal elements are missing, <30% differentiate any Filzkörper material. In all cases % refers to proportion of mutant embryos scored with a specific defect. The width of the denticle belts was estimated by averaging counts of denticles in the first row of abdominal segment A2.

Gastrulation was observed with bright-field optics in embryos that had been covered with a thin layer of Voltalef 3S oil.

In the complementation tests between any two alleles of *tld*, percentage survival of the mutant progeny in a cross was calculated from the ratio of actual survivors to the expected number. The number of mutant progeny expected to survive was estimated as half of the number of flies recovered carrying a balancer chromosome.

The following double mutants were tested: (1) *zen* with other ventralizing null alleles: zen^{w36}, srw^{B18} and zen^{w36}; tld^{B4} and scw^{S12}; zen^{w36} and dpp^{Hin46}; zen^{w36}. (2) Alleles with similar phenotypic strength: zen^{w36}, srw^{10K} and scw^{IG}; srw^{10K} and $dpp^{hin\text{-}r4}$; srw^{10K} and scw^{N5}; srw^{B18} and scw^{N5}; tld^{9B} and $dpp^{hin\text{-}r4}$, scw^{IG} and scw^{C13}; tld^{9B} and $dpp^{hin\text{-}r27}$, scw^{C13}. (3) Null allele combinations: scw^{S12}; srw^{B18} and scw^{S12}; tld^{10F} and srw^{B18}, tld^{10F} and dpp^{Hin46}; srw^{B18} and dpp^{Hin46}; tld^{10F} and dpp^{Hin46}, scw^{S12}. (4) Mutants affecting different regions: dpp^{Hin46}, twi^{ID} and scw^{S12}, twi^{ID} and sna^{IG}; srw^{B18} and twi^{ID}; zen^{w36}.

Antibody labelling

Immunological staining of whole-mount embryos for visualizing β-tubulin was carried out as described by Foe (1989). Staining for cyclin-A was carried out in an identical manner, except for the elimination of taxol prior to the fixation step. Monoclonal mouse anti-β-tubulin IgG supplied by Amersham was used to visualize the microtubules during cell division. The polyclonal antibody directed against cyclin A protein, was kindly provided by Dr P. O'Farrell. In both cases, appropriate RITC-conjugated secondary antibodies were used. Taxol was provided by the National Cancer Institute Natural Products Division. For the fate mapping studies, embryo collections were always done at 25°C on apple juice agar plates. Staging was done according to Campos-Ortega and Hartenstein (1985).

Whole mount in situ *labelling*

The plasmid used as probe for *sim* is a 2.8 kb cDNA (Thomas et al., 1988). The insert was an *Eco*RI fragment cloned into

pGEM-1. Gel-purified cDNA fragments were labelled with digoxigenin (~50ng DNA/labelling reaction) according to the protocol described in the Kit supplied by Boehringer Mannheim (Cat. 1093-657). Whole-mount in situs were done essentially as described by Tautz and Pfeifle (1989). Stained embryos were mounted in Permount (Fisher).

Transplantation of pole cells

The protocol for transplantation of pole cells described by Nüsslein-Volhard et al. (1985) was followed. Hatch rates and frequencies of mutant embryos were determined according to Nüsslein-Volhard (1977). Recipient embryos were produced by Oregon R females crossed with ovo^D males. Donor embryos were obtained from the following crosses: (1) $zen^{w36}/TM3,Sb$ females with $Df(3R)LIN/TM3,Sb$ males, (2) $srw^{B18}/TM3,Sb$ females with $Df(3L)e13/TM6$ males, (3) scw^{S12}/CyO females with $Df(2L)TW9/CyO$ males and (4) $tld^{6P1}/TM3,Sb$ females with $tld^{10F}/TM3,Sb$ males. In addition to scoring the fraction and phenotype of lethal embryos laid by a fertile female, the genotypes of the donor pole cells were confirmed by scoring the visible markers of adult progeny that survived in crosses between the host females mated to $zen^{w36}/TM3,Sb$, $srw^{B18}/TM3,Sb$, scw^{S12}/CyO and $tld^{10F}/TM3,Sb$ males, respectively.

Results

Cuticular markers of the dorsoventral pattern of wild-type larvae

In the segmented middle body region, the externally visible DV pattern of the *Drosophila* larva consists of the ventral setal bands and fine dorsal hairs separated by a lateral region comparatively free of cuticular specializations. Cells from the mid-dorsal and the mid-ventral regions of the blastoderm do not contribute to this cuticular pattern (see wild-type larva in Fig. 1A and fate map in Fig. 2; Lohs-Schardin et al., 1979). The ventralmost 20% of the embryonic cells invaginate as part of the ventral furrow and give rise to muscle and other mesodermal derivatives. On the dorsal side, 10% of the cells at cellular blastoderm stage become the amnioserosa, which subsequently contributes to the formation of the pericardial wall and the hypoderm (Technau and Campos-Ortega, 1986). In the terminal regions of the embryo, distinct cuticular structures are derived from specific positions along the DV axis on the blastoderm fate map (Jürgens et al., 1986, Jürgens, 1987). The antennal and maxillary sense organs, which occur in the head, and elements of the head skeleton (hs, in Fig. 1A), like the mouth hooks, cirri and the dorsal appendages, are derived from the dorsal and dorsolateral positions, respectively. Posteriorly, the spiracles and the Filzkörper (fk, in Fig. 1A), which are tracheal specializations, serve as markers for specific dorsal and dorsolateral positions on the blastoderm.

The phenotype of mutations causing ventral pattern deletions

The phenotypic effects of mutations in the genes *twi* and *sna*, have been described previously (Simpson, 1983; Grau et al., 1984; Leptin and Grunewald, 1990). The most striking defect is that homozygous *twi* and *sna* embryos do not form a ventral furrow. These embryos exhibit a characteristic "twisted" morphology upon differentiation (Fig. 1B), with occasional mismatches of the cuticular pattern along the ventral midline. Internally, they lack mesodermal derivatives (Leiss et al., 1988).

The cuticular phenotypes of mutations causing dorsal pattern deletions

Apparent null alleles of the genes belonging to the dpp group can be arranged in a phenotypic series in which one encounters a progressive loss of the amnioserosa and then the dorsal ectoderm, including dorsolaterally derived structures of the acron and the telson. Null mutations in *zen* and *srw* exhibit a weaker ventralizing phenotype (class II, Table 1) compared to those of *scw* and *tld* (class IV, Table 1), which represent moderately ventralized phenotypes (Fig. 1E,F,H,I). Complete loss-of-function mutations in *dpp* represent the strongest ventralizing phenotypes (class V, Table 1) caused by mutations in a zygotic gene (Fig. 1J and see below).

Null mutant embryos of *zen* and *srw* display loss of the dorsalmost pattern element, the amnioserosa. The anterior abdominal segments exhibit gaps across the ventral midline or misfusions across segment boundaries and may show a slight extension of ventral setal bands (Fig. 1E,F). The Keilin's organs, which occupy a ventrolateral position in each thoracic segment, are occasionally duplicated. Mismatches and fusions of the segmentally defined dorsal hairs occur at the dorsal midline. At the posterior end, the telson as well as the spiracles, the Filzkörper and the last abdominal segment do not evert. Head involution is affected, so that parts of the cephalo-pharyngeal skeleton are visible externally. Even the weakest mutants of this class show defects at the termini; the embryos have incompletely involuted heads and an altered telson morphology (data not shown).

Homozygous null alleles of *tld* and *scw* show a stronger phenotype, manifested in the absence of the amnioserosa and a reduction of the dorsal cuticle accompanied by an estimated 30% increase in width of the ventral setal belts in each segment. The ventrally placed Keilin's organs often show an increase from three to five sensory hairs per sensory organ. This phenotype is similar to that of partial loss-of-function alleles of *dpp* (Fig. 1G-I). Maxillary sense organs, that derive from a dorsolateral position on the blastoderm fate map (Jürgens et al., 1986), are absent. The antennal sense organs which arise from adjacent cells, in a relatively ventral position, are encountered only in a third of the mutant embryos. They are present singly or, if paired, on one side of the head only. Strong loss-of-function alleles of *tld*, *scw* and *dpp* suffer a loss of pharyngeal skeletal elements. The thorax is characteristically coiled (Fig. 1G-J). While the morphology of the thoracic segments may be a secondary consequence of torsion in the germband during gastrulation (see below), the loss of dorsal and dorsolaterally derived elements of the head skeleton are indications of the strength of the phenotype. As is typical of strongly

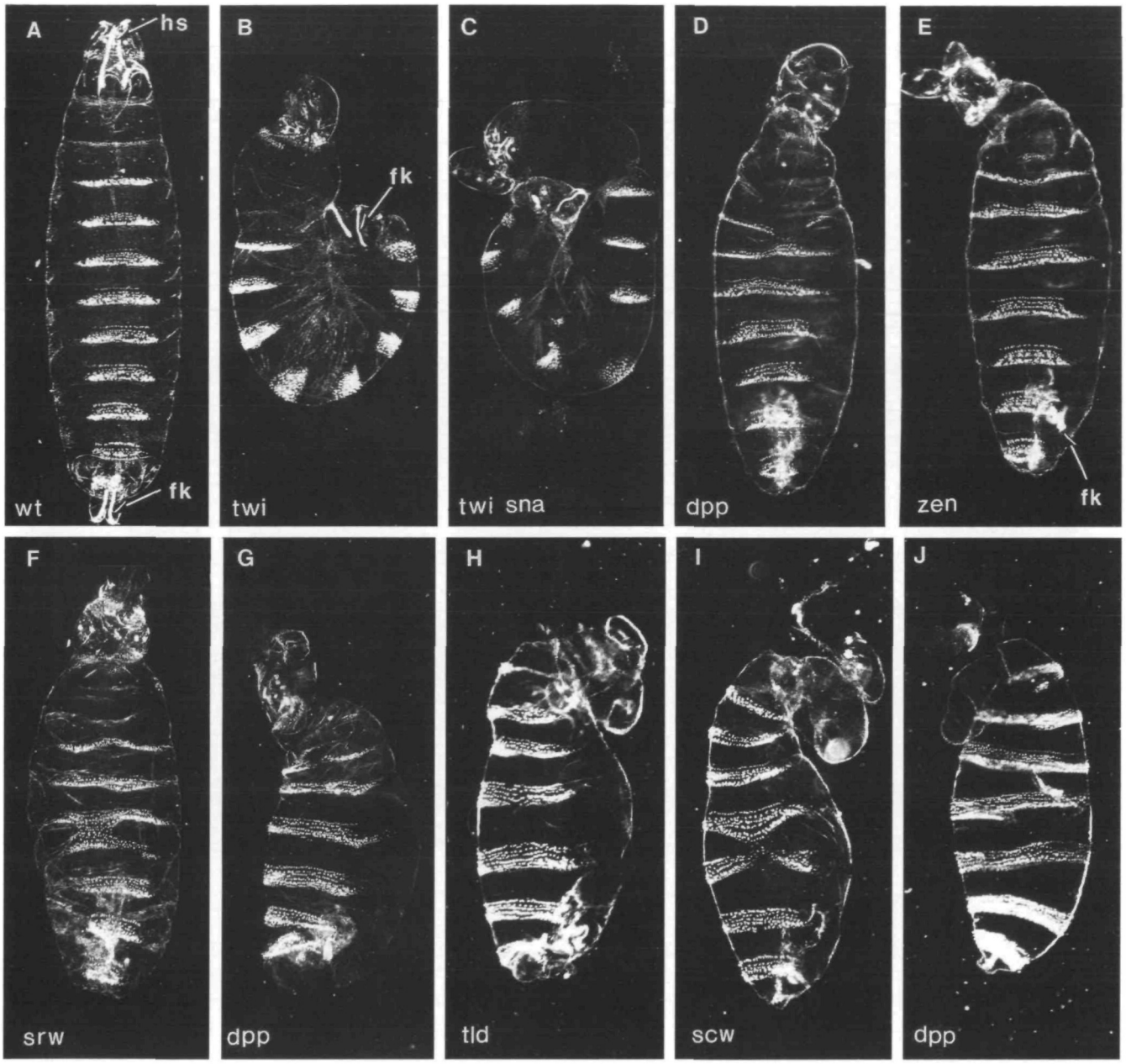

Fig. 1. Cuticular phenotypes of zygotic dorsoventral pattern mutants. Larvae are oriented anterior up and ventral side facing, unless mentioned otherwise. (A) Wild-type cuticle. Larva showing the normal width of the ventral denticle belts in each thoracic and abdominal segment. Chitinised mouthparts and the head skeleton (hs) are distinct anteriorly, as are the tracheal specialisations, the Filzkörper (fk), posteriorly. (B) Lateral view of a twi^{1D} mutant. The larval body is characteristically coiled. The head is disorganised but the Filzkörper are distinct. (C) Cuticle of a *Df(2R)twiS60*, sna^{11G} double mutant embryo. General morphology of the larva is the same as that in B, the ventral denticle bands in each segment are narrower. (D) $dpp^{hin\text{-}r4}/dpp^{hin\text{-}r27}$, (E) zen^{w36} and (F) srw^{B18} mutant larvae exhibiting a weak ventralized phenotype. Denticle bands in the thoracic segments are disrupted mid-ventrally. The head is not involuted and structures posterior to the eighth abdominal segment have not everted, as a result of which the Filzkörper are seen internalised. (G) $dpp^{hin\text{-}r27}/dpp^{hin\text{-}r92}$, (H) tld^{B4} and (I) scw^{S12} mutant larvae showing a moderately ventralized phenotype. Ventral denticle bands are extended compared to the wild-type embryo in A. In addition, the head structures are not involuted and the thorax is convoluted. Some dorsal epidermis is present and remnants of the Filzkörper are still evident. (J) Cuticle of a strongly ventralised dpp^{Hin46} embryo. The denticle bands are extended and encircle the larval body.

ventralized embryos, the terminal abdominal segment and the telson are pulled into the posterior end of the embryo during development. The dorsolaterally derived spiracles are often reduced to a single structure containing spots of Filzkörper material, present internally.

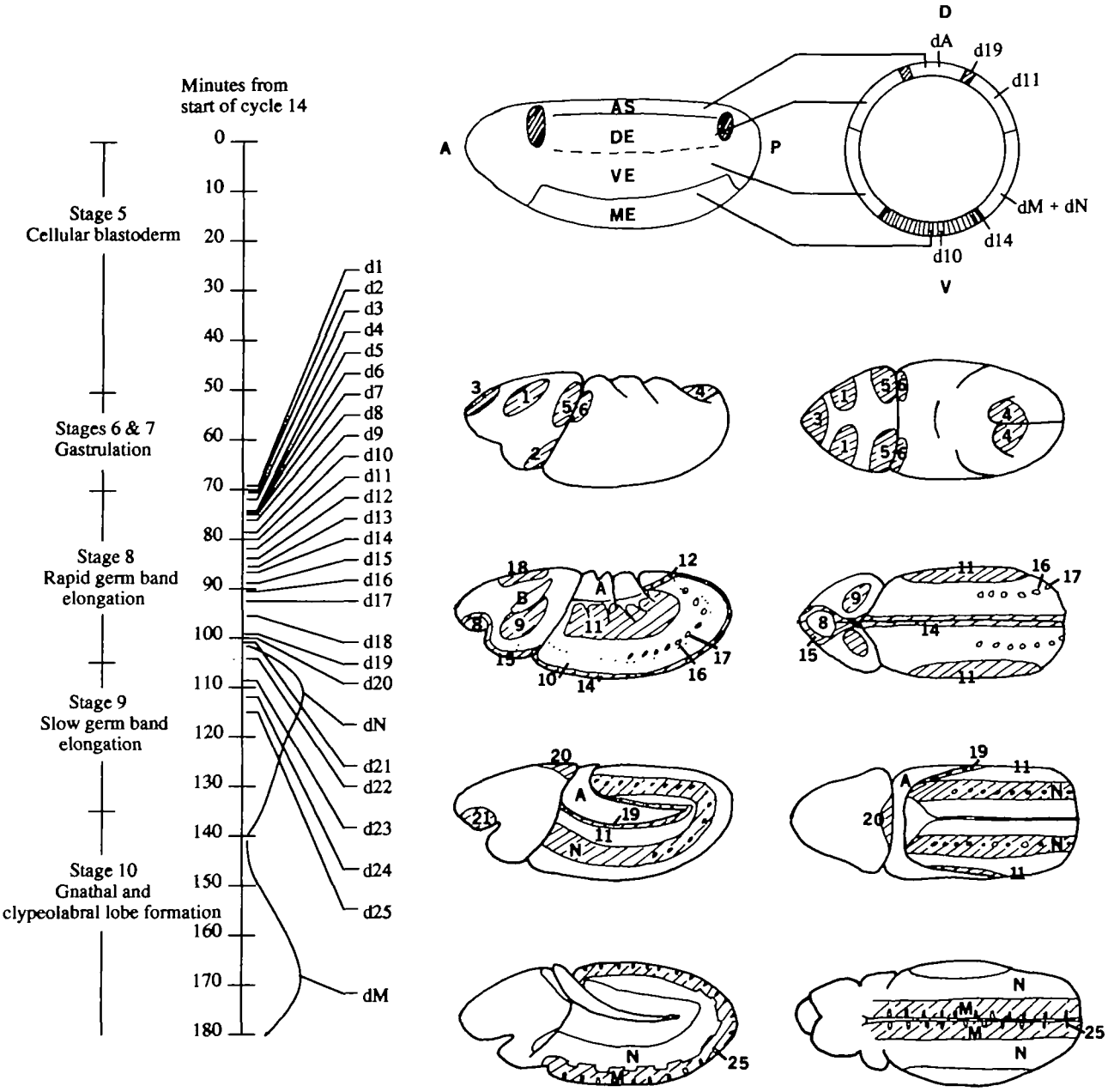

Fig. 2. Fate map of the cellular blastoderm embryo and the atlas of the mitotic domains projected onto gastrulating embryos at different stages. On top a lateral view and cross section of the fate map is schematised. In the cross section, the fate map in the middle body region has been correlated with the different mitotic domains along the dorsoventral axis. With the exception of δA (amnioserosa, AS) and δ10 (mesoderm, ME), the domains are bilaterally symmetrical, i.e. δ14 (mesectoderm), δM and δN (VE, ventral neurogenic ectoderm), δ11 and δ19 (DE, dorsal ectoderm and peripheral nervous system). The two hatched patches at the dorsolateral position in the fate map (lateral view), mark the anlagen of the antennal and maxillary sense organs, anteriorly, and the Filzkörper and spiracular openings, posteriorly. Schematic figures in the lower panel depict the cycle 14 mitotic domains as they appear at different stages of gastrulation (based on Foe, 1989; this work). Top to bottom, embryos at the beginning of stage 8, late stage 8, stage 9 and at stage 10, respectively. Embryos at left show a lateral view. Embryos depicted at right alternate dorsal and ventral views, although posterior to the cephalic region cells along the entire dorsoventral axis can be seen in a single plane, as the germ band flattens out and extends over itself like a ribbon and the amnioserosa folds back. Actively dividing domains at each stage of gastrulation are hatched. The numbering of the mitotic domains indicates the order in which they occur. Individual cells in these 25 domains divide in near synchrony, divisions in δN and δM are metasynchronous, while cells in δA and δB never divide after cycle 13. Domains δ16 and δ17 are reiterated in each abdominal segment in a segmentally repeated pattern. Ongoing morphogenetic movements reposition the domains relative to their earlier locations. The time line at the left margin of the figure indicates the time at which division occurs in each domain. The time axis is marked in minutes and zero refers to the start of the fourteenth interphase at 25°C.

The strongest ventralizing phenotype is represented by the complete loss-of-function alleles of the *dpp* gene, a strong indication that this gene plays a central role in pattern formation in the dorsal part of the embryo (Irish and Gelbart, 1987; see Table 1). Mutant embryos differentiate rings of ventral denticle belts around the entire DV axis and almost no dorsal hairs are seen (Fig. 1J). Dorsolateral pattern elements like the antennal and maxillary sense organs, which are associated with the cephalic cuticle, are missing. Mouth hooks, cirri and parts of the cephalo-pharyngeal skeleton derived from lateral positions on the blastoderm fate map (Jürgens et al., 1986) are also not seen (Fig. 1J). The absence of these structures in *dpp* embryos indicates a more severe pattern deletion compared to *scw* and *tld* null mutants. Posteriorly, remnants of Filzkörper material and disorganised rudiments of the spiracles can be distinguished in ~30% of the mutant embryos.

Gastrulation phenotype of the dpp group mutants

Mutant embryos at the loci *srw*, *scw* and *tld* show alterations in the morphogenetic movements of gastrulation similar to those described for *zen* and *dpp* (Irish and Gelbart, 1987; Rushlow and Levine, 1990). The earliest indication of an altered behaviour of cells on the dorsal side is seen in the shift of the normally lateral cephalic furrow to a more dorsal position in the mutant embryos. This is first apparent by 15 minutes after the start of gastrulation, i.e. 65-70 minutes into cell cycle 14. Later in development the cephalic fold appears as a deep dorsal cleft in mutant embryos (as seen marked with arrowheads in Fig. 7F-H). Similar to wild-type embryos, the germband in mutant embryos initially extends dorsally and anteriorly. However, instead of remaining on the dorsal surface, the extending germband invades the interior of the embryo (as seen in Fig. 7A,D,E,H; compare position of arrows marked 'gb' in normal and mutant embryos at different times in development). The defective movement of the germband may be due to the loss of the amnioserosa and the fact that the dorsalmost cells in these mutants have acquired the lateral fate of the dorsal ectoderm (see below). The dorsal shift in the position of the cephalic fold and the failure of normal germ band elongation are consistent features of mutations in the dpp group genes, although these effects vary in severity. Interestingly, even mutants showing a weak cuticular phenotype, i.e. zen^{w36}, show a marked alteration in the position of the cephalic furrow (Rushlow and Levine, 1990; this work). Most movements associated with normal head involution fail to occur. The deep dorsal cleft persists through embryogenesis, effectively disconnecting the gnathocephalic regions from the thoracic and abdominal regions of the developing embryo. This could explain why a contiguous midgut is never formed despite the formation of an anterior and posterior midgut, the hind gut and associated structures. The observation that the terminal abdominal segment and the telson remain pulled in at the posterior end of the embryo in the differentiated larva, may be a consequence of the defective germband extension in ventralized mutant embryos.

The ventralizing genes do not encode any maternally acting components

The complete loss-of-function phenotype of zygotic lethals is normally inferred from the homozygous mutant embryos obtained from heterozygous parents. However, the possibility exists that the gene is transcribed during oogenesis and the gene product is present in the egg, thus weakening the null zygotic phenotype, or that the gene has another function at other times in development. To test these possibilities, we constructed females with germlines that were homozygous mutant for strong alleles of *zen*, *srw*, *scw* and *tld* and compared their progeny with those from heterozygous females. The genes *twi*, *sna* and *dpp* have been previously shown to be required only in the zygote for normal embryonic development (Frohnhöfer, 1982; Irish and Gelbart, 1987).

To obtain germline-soma chimeras of the mutants, we transplanted pole cells from mutant donor embryos into recipient embryos carrying the dominant female-sterile mutation *ovoD* (see Materials and methods; Busson et al., 1983). *ovoD*/+ females do not lay eggs due to a cell-autonomous defect of the germline, but are capable of producing eggs from transplanted donor germ cells (Perrimon, 1984). The genotype of the germline in chimeric females was determined by the frequency of mutant embryos in crosses with heterozygous mutant males. Fertile females produced either no mutant embryos (class I), about 25% (class II) or about 50% (class III) mutant embryos; dependent on whether they had been implanted with wild-type, heterozygous or homozygous mutant germ cells. Females belonging to class III were recovered for *zen*, *srw*, *scw* and *tld* and they produced homozygous mutant embryos that did not differ in their cuticular phenotype from those produced in a cross between heterozygous mutant parents (Table 2). Thus these genes are apparently not required for normal development of the germline, nor do they show a significant maternal influence on embryonic development.

Patterned mitoses reveal discrete domains of cells along the dorsoventral axis

We have used the patterned mitoses in cell cycle 14 to follow the altered development of mutant embryos. We discuss below the pattern of mitosis in a wild-type embryo. The first 13 cleavage divisions in a fertilized embryo are essentially synchronous (Foe and Alberts, 1983). Following cellularization, groups of cells enter mitosis 14 in an established spatial and temporal sequence, allowing the surface of the embryo to be mapped into domains of mitotic activity (Hartenstein and Campos-Ortega, 1985; Foe, 1989). These mitotic domains occupy specific positions along the two major body axes of the embryo, suggesting that a significant level of specification of the embryonic pattern has already occurred at this stage. The observation that

Table 2. *Analysis of pole cell transplantation experiments to determine germline dependence of ventralizing genes*

Donor*	No. of eggs injected	No. of adults recovered	No. of adult females	No. of fertile females	Genotype of donor pole cells		
					Class I	Class II	Class III
zen	206	97	39	14	0**	8	6
srw	198	110	44	16	6	6	4
scw	235	101	55	14	3	7	4
tld	289	130	56	12	0**	8	4

*See Materials and methods for exact allele and genotype of donor crosses.

Class I, homozygous balancer; Class II, heterozygous mutant; Class III, homozygous mutant. Refer to Materials and methods, and Results section.

**In donor crosses when both genotypes were balanced with *TM3,Sb*, no females were recovered of this class. Presumably the *TM3* chromosome results in germ line sterility in a homozygous condition.

cells within a given mitotic domain share distinct attributes, such as cell morphology, morphogenetic behaviour and eventually differentiated cell fates (Foe, 1989), has allowed us to use mitotic domains for the purpose of fate mapping mutant embryos. Cells in different stages of mitosis were visualised in fixed whole-mount embryos by staining with an antibody directed against β-tubulin (see Materials and methods; Karr and Alberts, 1983).

A schematic version of the 25 mitotic domains that are seen during division cycle 14 in a normal embryo, is presented in Fig. 2 (based on Foe, 1989). Cells in δA and δB do not divide after completing cycle 13. The numbering of domains indicates the sequence in which they enter mitosis (refer to the time line). The transverse section in Fig. 2 correlates the domains of division encountered along the DV axis with the fate map of cells in the middle body region. Domains δA and δ10 straddling the dorsal and the ventral midline, respectively, correspond to the prospective amnioserosa and the mesoderm. The adjacent domains δ19 and δ11, which are bilaterally symmetrical, correspond to the dorsal ectoderm. Cycle 14 divisions in the ventral neuroectodermal region (δN and δM), occur later than in the rest of the cells and are typically not synchronous.

The mesectodermal domain is shifted ventrally in twi *mutants and expanded in* sna *mutants*

In embryos mutant for *twi* and *sna*, ventrally located cells do not invaginate to form a normal ventral furrow (Fig. 3B, compare with wild-type embryo in Fig. 3A). However, the earliest visible alteration in the mitotic patterns of these mutants is a significant delay in the division of cells belonging to δ3 and δ4. Normally δ3 occupies a median position at the anterior tip of the embryo and δ4 forms the posterior tip of the elongating germband (Fig. 3C). This delay in mitosis is restricted to δ3 and δ4. The paired domains δ1, δ5 and δ6 appear at the normal times (Fig. 3D). In mutant embryos, cells in δ3 and δ4 divide about the time δ8 divides, i.e. about 5 minutes later than in wild-type embryos (not shown). The functional relevance of this effect on domains that comprise cells deriving from the termini is not obvious. But it is interesting that both *twi* and *sna* are transiently expressed in terminal regions of the embryo, where their expression is regulated by maternal genes of the *torso* group (Klingler et al., 1989; Leptin and Grunewald, 1990; Ray et al., 1991).

In both *twi* and *sna* mutants, there are no divisions on the ventral side that correspond to the mesodermal domain. In wild-type embryos, the presumptive mesodermal cells divide en bloc as part of δ10, followed shortly by divisions in δ14, which consists of a single row of cells on either side of δ10. Cells in δ14 correspond to the mesectoderm and occupy a mid-ventral position in the gastrula after invagination of the mesodermal primordia (Fig. 3E). Divisions in δ10 cannot be seen in uncleared whole-mount wild-type embyos, as these cells have invaginated prior to division in this domain.

The most striking difference between *twi* and *sna* mutants is encountered in the position of the δ14 domain. In *twi* embryos at stage 8 (Campos-Ortega and Hartenstein, 1985), cells in δ14 comprise two irregular rows of dividing cells (Fig. 3F). Notably, these rows are still separated by a mid-ventral strip of non-dividing cells, which would have made up δ10 in a wild-type embryo. The position of δ14 appears to be shifted closer to the ventral midline by about two cells on each side.

In contrast to *twi* embryos, the *sna* mutants show groups of dividing cells in the mid-ventral region (see short arrows in Fig. 3G,H). Although the position of these dividing cells corresponds to that of the mesodermal domain δ10, the timing of division does not. The progeny from these divisions do not invaginate. These ventral cells in *sna* embryos divide after those in the dorsolateral domain δ11 (Fig. 3G), and about the time of division in δ14 (Fig. 3H). Therefore, we suggest they represent an expansion of δ14 in the *sna* mutant, such that this domain now includes the mid-ventral cells corresponding to δ10 in a normal embryo.

The domains δM and δN, which occupy ventrolateral positions on either side of δ14 in a wild-type embryo at the beginning of stage 9 (Fig. 3I), are separated by a broad swathe of ventral cells in *sna* embryos (marked with short arrows in Fig. 3K). The extra cells in the ventral region of a *sna* embryo, compared to that in a wild-type or a *twi* mutant, most likely correspond to the progeny of the extended δ14 domain in *sna* mutants (Fig. 3I-K). This ventral region is delineated by cells belonging to δM which, even prior to division, can be recognised by their characteristic orientation perpen-

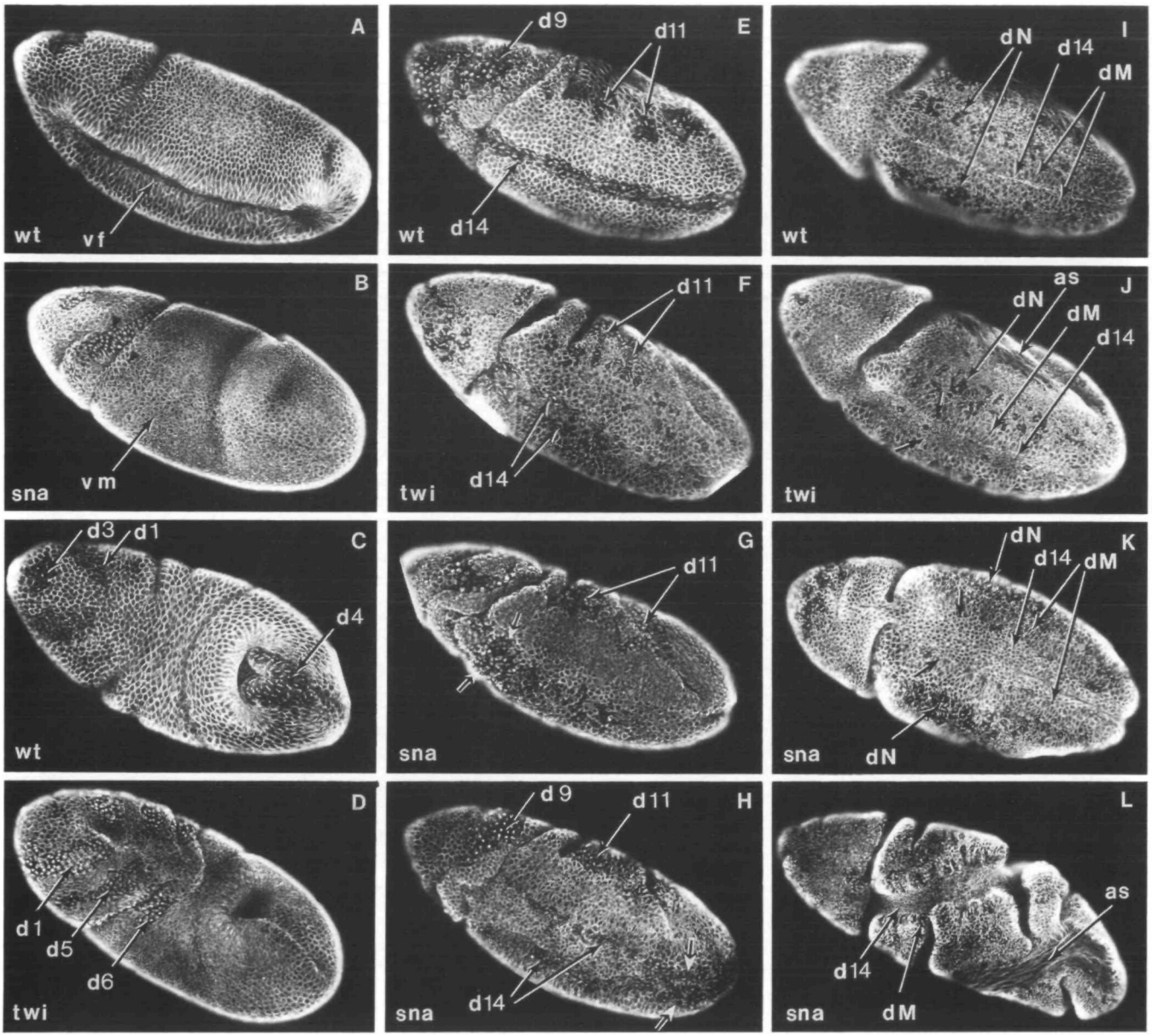

Fig. 3. Mitotic domains in mutants affecting ventral pattern. Embryos have been stained for β-tubulin. Microtubules are organised as bipolar spindles in dividing metaphase nuclei and exhibit a ring-like appearance in cells at interphase, as in the cells marked with arrowheads in B. All embryos are oriented so anterior is at top left corner. At the start of gastrulation, a wild-type embryo (A) forms a ventral furrow (vf) which is conspicuously missing in the *sna* embryo (B). The ventral midline (vm) is marked. Dorsal view of a wild-type (C) and *twi* embryo (D) at the beginning of stage 8. Domains δ3 and δ4 are missing in the mutant, although it is ~5 minutes older than the embryo in C. Cells in δ1, δ5 and in δ6 are dividing normally. Ventrolateral views of wild-type (E), *twi* (F) and *sna* mutants (G, H) at stage 8. In the wild-type embryo ventral furrow formation brings cells in the adjacent δ14 domains close together at the ventral midline (E). In *twi* embryos, the mesodermal domain, δ10, is missing and two irregular rows of cells comprising δ14 are seen occupying a ventral position among cells which have not invaginated (F). In *sna* embryos patches of mid-ventral cells (marked with short arrows) divide shortly after divisions in the dorsolateral δ11 (G), and in time with cells belonging to δ14 (H). δ9 occurs at its normal dorsolateral position (E, H). In the wild-type embryo at stage 9 (I), δ14 is flanked by the paired δM and δN in ventrolateral positions. Cells in δM can be recognised prior to division by their characteristic orientation perpendicular to the ventral midline defined by δ14. In *twi* (J) and *sna* (K) embryos at stage 9, additional cells at the ventral side (marked with short arrows) separate δM in each half of the embryo. (L) Ventral view of a *sna* embryo at stage 10 showing division in δM, which exclude a stripe of cells situated mid-ventrally. The germband is considerably twisted, which is reflected in the altered position of the amnioserosa (as). The alleles shown are *Df(2R)twiS60* and sna^{IIG}.

dicular to the long axis of the embryo (see δM in Fig. 3K,L). Comparatively, in *twi* embryos, δM appears to have moved closer ventrally, suggesting that, in the absence of δ10, the boundary of δM is also shifted in a coordinated manner to the shift in δ14 (Fig. 3J).

Domains δ19 and δ11 along the DV axis appear normal and a normal amnioserosa is formed (amnioserosa marked in Fig. 3J,L). Germband extension occurs in *twi* and *sna* mutant embryos, but the morphology of the germband is distorted by deep folds and considerable twisting (Fig. 3L). This may be a consequence of the lack of ventral furrow formation combined with the occurrence of normal divisions in ventrolateral cells.

We attempted to determine whether all ventral cells occupying the position of the deleted mesodermal anlagen in the *twi* and *sna* mutants complete cycle 14 divisions, using an anti-cyclin A antibody. During cell cycle 14, cyclin A protein accumulates at the same rate in all cells. However, it is completely and rapidly degraded during each metaphase and reaccumulates prior to subsequent cell cycles (Lehner and O'Farrell, 1989, 1990). This allows us to identify all the cells that have divided during a given period in time and therefore lack cyclin A, instead of restricting the window only to cells dividing at the particular moment that the embryo was fixed (as in the case of embryos stained for β-tubulin).

Fig. 4 shows wild-type, *twi* and *sna* mutant embryos at stage 8, in which δ11 and δ14 divisions have just occurred. In the wild-type embryo, the paired δ14 are adjacent since the mesoderm has invaginated. In the *twi* embryo, the corresponding two rows are separated by a stripe of ventral cells that would have contributed to the mesodermal domain. The width of the region is smaller than the normal distance between mesectodermal cells, indicating that δ14 has in fact shifted ventrally (Fig. 4B). Prior to gastrulation the mesodermal anlage is about 18 cells wide ventrally (Thisse et al., 1988). However, δ14 does not occupy the ventralmost position in *twi* embryos as they show a random distribution of cells at the ventral midline, which have not divided. A study of older embryos reveals that several cells in the mid-ventral region do not divide, at least until the end of stage 9, at which time mesodermal cells in normal embryos would have entered cycle 15 (not shown). This implies that a subset of ventral cells do not behave either as presumptive mesodermal cells or as the lateral mesectodermal cells (schematized in Fig. 9). In contrast to *twi* embryos, all ventral cells in a *sna* mutant have completed one round of division as part of δ14 at the end of stage 8 (Fig. 4C).

Corroborative evidence for the altered identity of ventral cells in *twi* and *sna* mutants comes from the distribution of the *sim* transcripts (Fig. 4D-F). The *sim* probe labels the mesectodermal cells that subsequently give rise to specific glial cells in the ventral nervous system (Foe, 1989; Crews et al., 1988). In normal embryos, *sim* is expressed in two rows, one on either side of the presumptive mesoderm, separated by 17-18 cells on the ventral side (Thomas et al., 1988). The two rows of cells expressing *sim* occupy adjacent positions in the embryo following the invagination of the mid-ventral cells (Fig. 4D). In *twi* mutants, *sim* expression is separated only by about 8 cells in an early stage 7 embryo (Fig. 4E). Additionally, the initial expression of *sim* is delayed and levels of expression are lower. In *sna* mutants, *sim* is expressed as a band along the ventral midline of the embryo, including the cells that would form the mesoderm in a wild-type embryo (Fig. 4F), confirming the identity of the mid-ventral cells.

The observation that the *twi* and *sna* genes affect the fates of the ventral cells in a contrasting manner suggests that they are responsible for different aspects of ventral pattern specification. In wild-type embryos, both genes are expressed in a largely overlapping subset of ventral cells (Thisse et al., 1987; Leptin and Grunewald, 1990; Kosman et al., 1991). Neither *twi* nor *sna* affect the initiation of expression of the other (Leptin and Grunewald, 1990; Ray et al., 1991; Kosman et al., 1991). One interpretation of the results described in the preceding sections is that *twi* may be required to specify the mesoderm, while the function of *sna* may be to repress mesectodermal fates.

In the double mutant *twi sna*, there are no divisions corresponding either to δ10 or to δ14 in a stage 8 embryo which shows normal δ11 divisions on the dorsal side (Fig. 5A). The domain δ9, which normally occupies a lateral position anterior to the cephalic fold, is continuous across the ventral midline, as is the cephalic fold itself (Fig. 5A, compare with embryo in Fig. 3E). Additionally, no *sim* expression is seen in the double mutant (Fig. 5B). Domains that occur in relatively lateral and dorsal positions like δN, δ11, δ19 and δA appear normal (only δN shown in Fig. 5C, D). However the ventrolateral domain δM, which normally flanks the mesoderm and the mesectoderm, is affected. The ventral boundary of the paired domain δM is not established, thus δM appears continuous across the ventral side. Cells in this domain, particularly at the mid-ventral region, do not behave normally (designated δM*, Fig. 5F). In wild-type embryos, cells belonging to δM exhibit a characteristic orientation of the mitotic spindle, perpendicular to the long axis of the embryo (Fig. 5E). Cells in δM* never acquire this characteristic of δM cells and only a subset divide, in an apparently random pattern. The large size of several ventral cells in mutant embryos at late stage 10 indicates that they have not divided at a time when adjacent cells, corresponding to δN in a normal embryo, have completed division and cells in dorsal regions have entered their fifteenth division cycle (Fig. 5E, F).

In *twi sna* embryos stained for cyclin A, we have confirmed that a larger portion of mid-ventral cells, compared to that in *twi* mutants alone, do not divide up to the end of cycle 14 (not shown). In these embryos, most of the cells occupying the normal position of δM do complete cycle 14, thus the aberrent behaviour appears to be restricted to cells from the deleted mesodermal and mesectodermal anlagen (see schematic version in Fig. 9). Despite their contrasting effects on mesodermal specification, *twi* and *sna* must

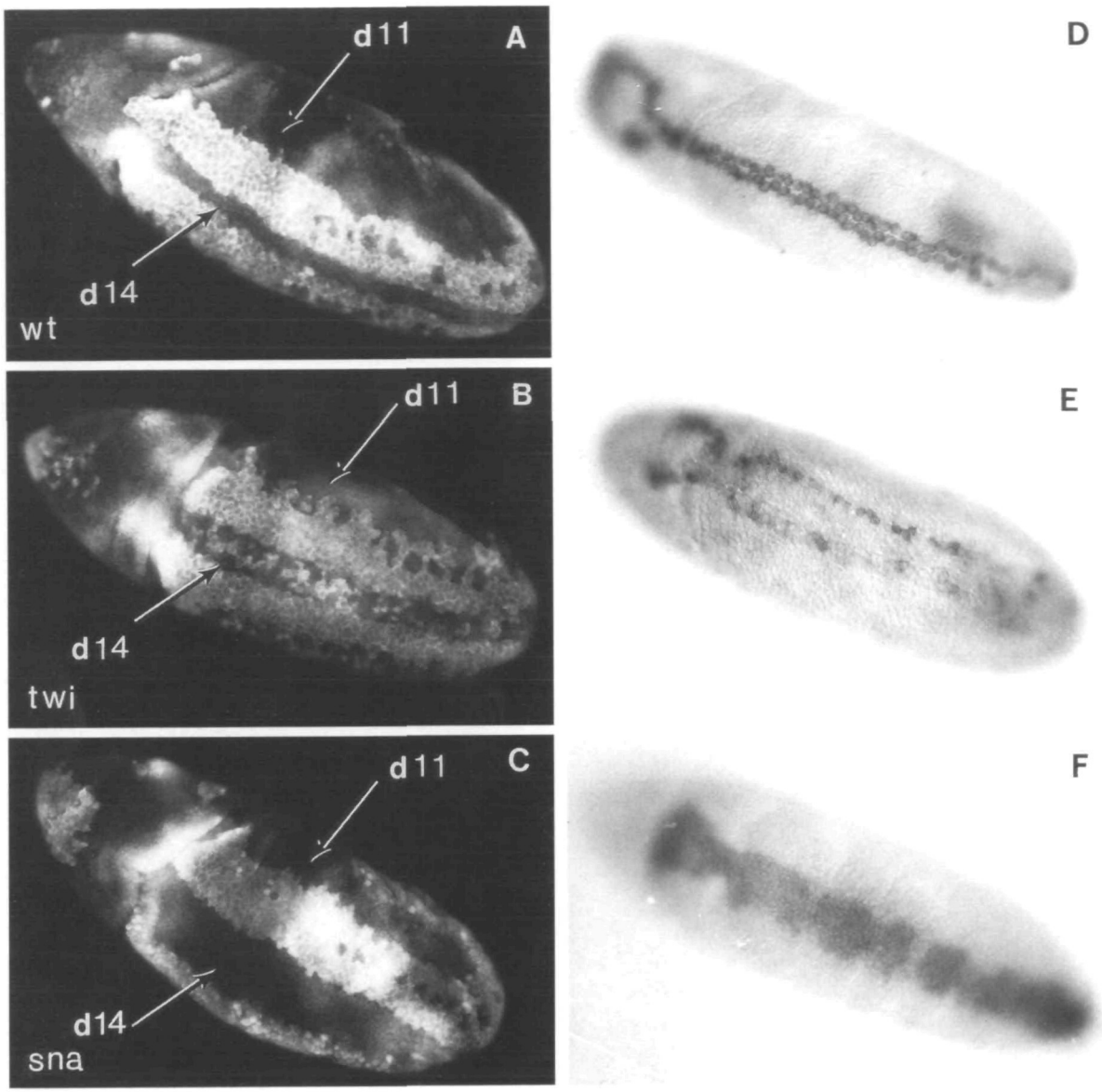

Fig. 4. Comparison of division in the mesectodermal domain (δ14) with the pattern of *sim* expression. Panel on left shows embryos stained for cyclin A protein, the panel on right shows in situ localization of *sim* transcripts in whole mounts. Wild-type (A, D), *Df(2R)twiS60* (B, E) and sna^{11G} mutants (C, F) at stage 8 are shown at left; embryos in right panel are at stage 7. Embryos are oriented so anterior is at top left corner and ventrolateral or ventral surface is facing. Cells with accumulated high levels of cyclin have not yet embarked on cycle 14 divisions, while those with no cyclin have just divided. In wild-type embryos (A, D), ventral furrow formation brings the paired ventrolateral domains δ14 (and the mesectodermal cells expressing *sim*) to the apparent mid-ventral position. The absence of this event in the mutants allows us to visualize the altered fate of the prospective mesodermal cells. In *twi* mutants (B) the δ14 domains are shifted closer to the ventral midlne. The *twi* mutant embryo at stage 7 (E), shows a similar ventral shift in the position of the cells expressing *sim*, which are separated by 7-8 cells compared to 17-18 cells in normal embryos (Crews et al., 1988). The expression is irregular as is the appearance of the δ14 domains in (B). In *sna* embryos (C), a broad stripe of ventral cells including the cells which normally give rise to the mesoderm, divide as δ14. Correlating ectopic expression of *sim* is seen in the ventral cells in (F). Cells in δ14 are identified on the basis of their relative position and/or timing of division, which normally follows division in dorsal cells belonging to δ11 by ~5 minutes (A- C).

cooperate in some aspect of their function, so that in the absence of both genes *sim* expression is lost and the mesectodermal anlagen is deleted in addition to the mesoderm (schematized in Fig. 9). Further, there is a more severe cuticular phenotype of the double mutant compared to either single mutant alone (Fig. 1B, C; *sna* embryo not shown), indicating that the combined absence of both *twi* and *sna* function may also affect the specification of the mesectoderm-neuroectoderm border.

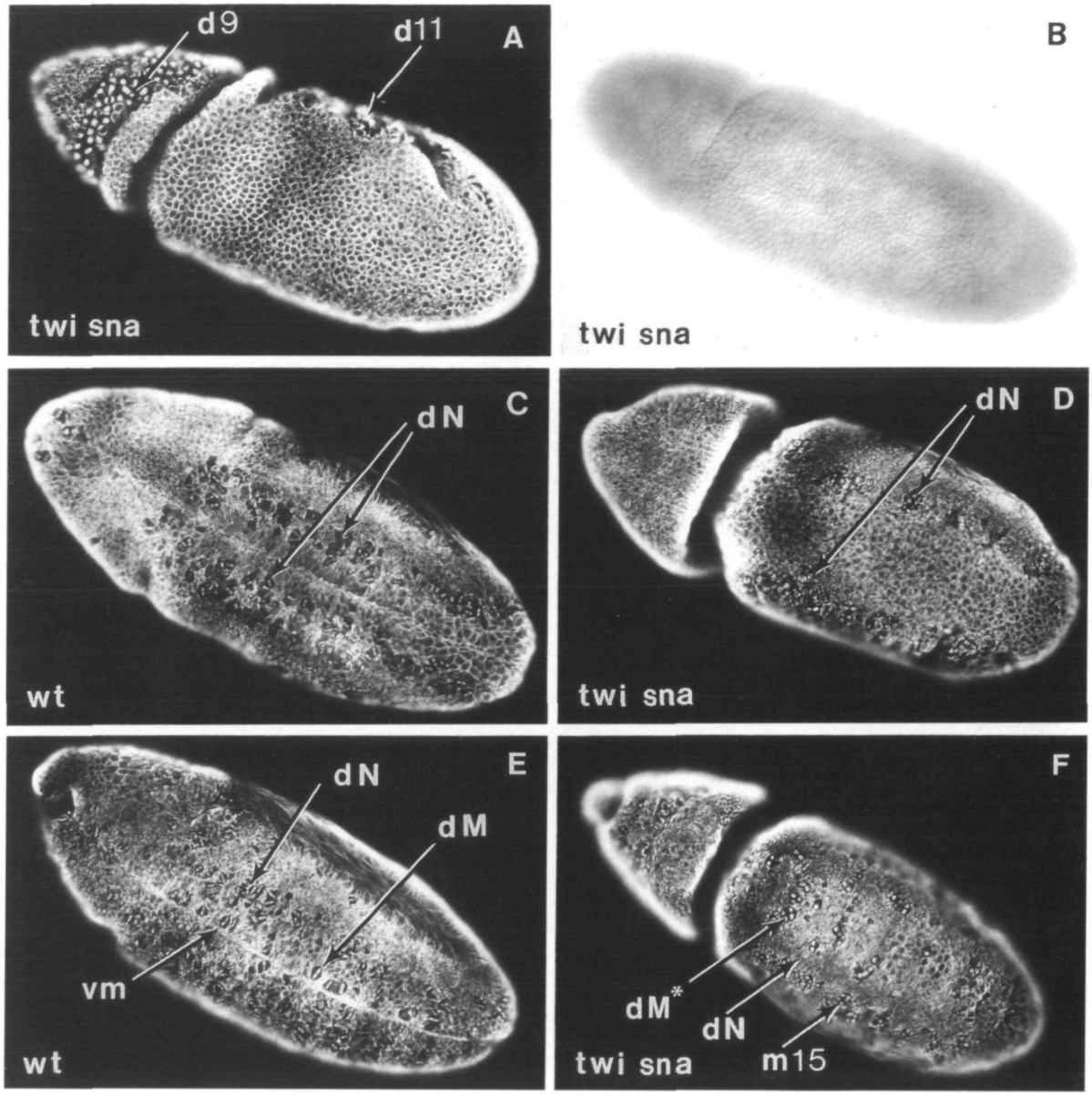

Fig. 5. Absence of specification of mesoderm and mesectoderm in *twi, sna* double mutant embryos. All embryos are stained for β-tubulin, except the embryo in (B) which is hybridized with the *sim* cDNA. Orientation is anterior at top left corner and ventral view facing. Double mutant *Df(2R)twiS60, sna*^{IIG} embryos are shown in A, B, D, F and wild-type embryos in C, E. In a double mutant embryo at stage 8 (A), there are no δ10 (mesodermal) divisions. δ11 occurs normally, but δ9 domain extends ventrally and comprises more cells than in normal embryos (wild-type embryo at the same stage shown in Fig. 3E). Divisions in δ14 (the mesectodermal domain) are absent (A), as is *sim* expression (B). In the double mutant at stage 9 (D), the neuroectodermal domains dN occur at their normal positions in each half of the mutant embryo, but appear further apart than in wild-type (C), because of the lack of ventral furrow formation. (E) A wild-type embryo at stage 10 shows cells in δM dividing with their characteristic orientation of the mitotic spindle, perpendicular to the ventral midline (vm). In a late stage 10 mutant embryo (F), a few ventral cells divide in an uncharacteristic manner (marked δM*), at a time when lateral cells in δN have completed division. Dorsal cells at the edge of the germband are beginning their fifteenth mitosis (m15). Note the large size of cells in the mid-ventral region, that have not divided.

Mutations in the dpp group genes delete dorsal cell fates and cause expansion of ventrolateral mitotic domains

Loss-of-function alleles of *tld*, *scw* and *dpp* produce cuticular defects more severe than those encountered in *zen* and *srw* mutants. A similar gradation can be seen in the extent to which the mitotic pattern is altered in these mutants. The *zen* mutants show the most restricted alterations in the pattern of mitosis, while null mutations in *dpp* affect divisions in a much larger

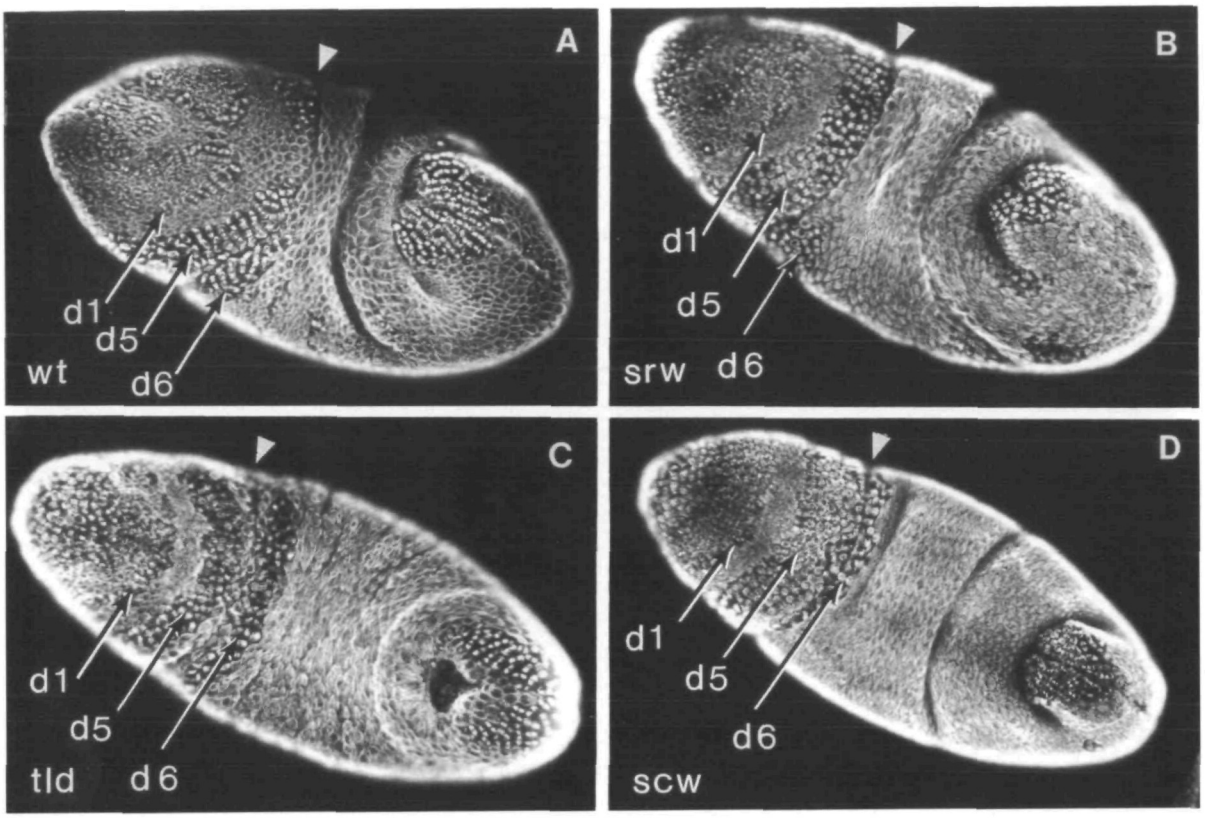

Fig. 6. Changes in cell fate in ventralized mutant embryos. Wild-type (A) and mutant embryos, srw^{B18} (B), tld^{9B} (C), scw^{S12} (D) at stage 8 have been stained for β-tubulin to show the dorsal shift in position of mitotic domains which normally occur at dorsolateral positions. Orientation is anterior at top left corner and dorsal side facing. The dividing cells in the wild-type embryo (A) belong to paired domains δ1 and δ5, which occur anterior to the cephalic fold, and δ6, which occurs posterior to the cephalic fold, each separated by a zone of non-dividing mid-dorsal cells. In the weakly ventralized *srw* mutant (B), δ1 and δ5 are continuous across the dorsal midline. In the more strongly ventralized *tld* mutant (C), δ6 has shifted dorsally as well. In *scw* embryos (D), δ6 is continuous and in addition, considerably reduced. (Fig. 6A was kindly provided by V. Foe.)

region. Domains δ1 and δ5, which occur on the dorsal surface anterior to the cephalic fold, and δ6, which occupies a similar position posterior to the cephalic fold, are excellent markers for such an analysis (Fig. 6A). In all the ventralizing mutants, the paired domains δ1 and δ5, normally distinct on either side of the dorsal midline, merge across the dorsal surface of the embryo as part of a single domain (Fig. 6B-D). The unpaired domains δ18 and δ20, which normally occur at the dorsal midline, are absent.

In wild-type embryos, the dorsal boundaries of δ1 and δ5 are closer than those of δ6, which occupy a comparatively lateral position. These domains are the first to appear as continuous domains in weak ventralizing mutants like *zen* and *srw*, only subsequently followed by the merging of δ6 in more severe ventralizing mutants like *tld* and *scw* (Fig. 6B-D). In *scw* mutants, the size of the fused δ6 is significantly reduced (Fig. 6D), and in the stronger *dpp* embryos the entire δ6 is missing (schematized in Fig. 9). The observation that δ6 is eliminated in the strongest ventralized mutant *dpp*, while the domains δ1 and δ5 are still present, is consistent with the fact that the lateral boundaries of δ6 are at a more dorsal position than those of δ1 and δ5.

In the middle body region, null mutants of each gene belonging to the dpp group lack the amnioserosa. Normally the dorsalmost cells constitute δA and do not divide after completing their thirteenth nuclear division cycle (Fig. 7B-D). As development proceeds these cells acquire the characteristic squamous morphology of the amnioserosa. In both *zen* and *srw* embryos, cells at the mid dorsal region divide in synchrony with cells in δ19 and δ11, the dorsolateral domains that occupy positions adjacent to δA (Fig. 2). Domain δ11, although considered one single domain, originates at five independent foci along the length of the germband and eventually forms a contiguous dorsolateral stripe of dividing cells in stage 8 embryos (Fig. 7A,B). In *zen* mutants divisions in δ11 begin normally, but later extend dorsally into the prospective δA (Fig. 7E,F). The mid-dorsal cells excluded from divisions in the extended δ11, are seen to divide in time with divisions in δ19, the narrow domain that normally forms a boundary between δA and δ11 (Fig. 7C,G). It is possible to identify δ19 cells, as they divide at the same

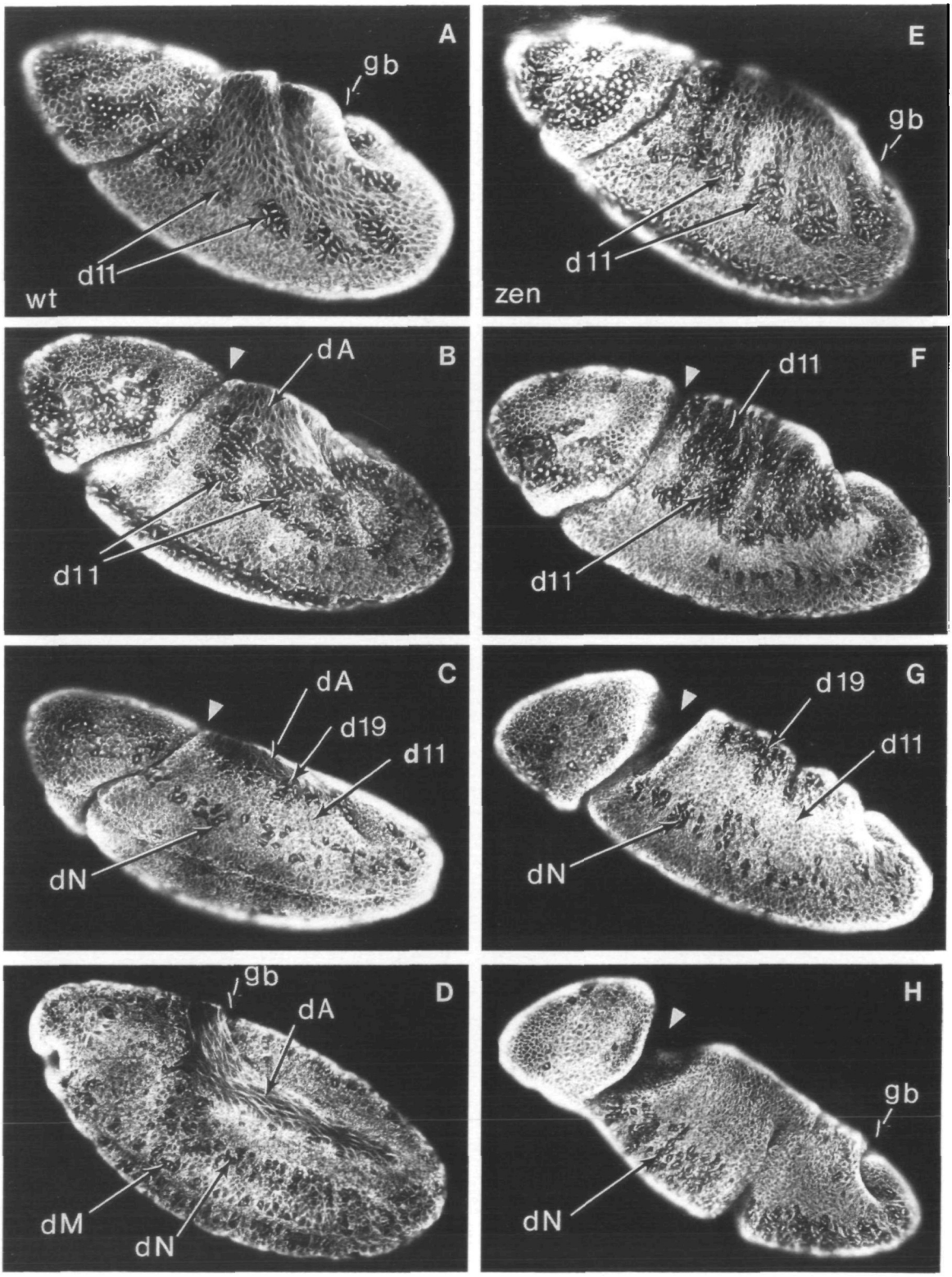

time as cells in δN. These observations indicate a shift in the division pattern of *zen* mutants, so that the cells in the mid-dorsal region (both anterior and posterior to the cephalic fold) behave as if they derive from lateral positions and belong to domains δ1, δ5 and δ19 at corresponding positions along the AP axis (schematized in Fig. 9). Cells on the ventral side divide normally as parts of δN and δM, the two domains that constitute the ventral neuroectoderm (Fig. 7D,H).

Mutations in *srw* show effects similar to those in *zen* mutants, with one exception. As in the *zen* mutant, δA is missing and there is a dorsal shift in the position of δ11 and δ19. However the expansion of δ11 does not occur after a significant delay, as in the case of *zen*

Fig. 7. Mitotic domains in wild-type and *zen* mutant embryos. Embryos at different stages of gastrulation have been stained for β-tubulin to visualize mitotic domains during cycle 14. Panel at left shows wild-type embryos (A-D) and at right, zen^{w36} mutants at comparable stages (E-H). Orientation is anterior at top left corner and lateral view facing. Germ band extension is affected in mutant embryos. The arrow 'gb' marks the position of the posterior end of the germ band in embryos at the beginning of stage 8 (A, E) and at stage 10 (D, H). The white arrowheads mark the cleft formed as the result of a dorsal shift in the position of the cephalic fold in ventralized mutants compared to normal embryos (B, C, F-H). At the beginning of stage 8, groups of cells constituting the early δ11 domains divide in both wild-type (A) and mutant embryos (E) at dorsolateral positions. As gastrulation proceeds in wild-type embryos (B), δ11 extends to forms a continuous domain along the anterior-posterior axis, excluding cells at the mid-dorsal position (δA). In a comparable stage *zen* mutants (F), the wave of division in δ11 extends dorsally, enlarging δ11 and largely eliminating δA. In wild-type embryos at late stage 8 (C), a narrow region (δ19) lateral to δA, divides at the same time as divisions in the ventrolateral domain, δN. In similar stage *zen* mutants (G), the position of δ19 is shifted dorsally replacing δA. (D) and (H) show wild-type and mutant embryos at stage 10 in which the remainder of the cells in δN and δM are dividing. Domain δM is obscured in the embryo in (H).

mutants. We believe this may reflect a subtle difference in the timing of action of the two genes. In addition, it appears that the position of δ19 is shifted further dorsally (schematized in Fig. 9). As in the case of *zen* embryos, no changes in the boundaries of more ventral domains were observed.

In *tld* and *scw* embryos, the dorsalmost cells in the middle body region divide as part of δ11. Thus, not only are δ1, δ5, δ6 continuous along the dorsal midline, but so is δ11, completely eliminating δ19 and δA. Unlike in *zen* and *srw* mutants where the shift in δ1 and δ5 affects only the dorsal boundaries of these domains, cell counts across the width of δ6 and δ11 in *tld* and *scw* mutants indicate that the shift affects the ventrolateral boundaries of these domains as well (Fig. 6C,D and schematic version in Fig. 9). In other words, the entire domains have shifted to a more dorsal position. In the segmented region of the embryo, the dorsal shift in position of δ6 and δ11 is coordinated with an expansion of the ventrolateral domains δN. Since divisions in the latter domain are normally not synchronous and occur over a total period of 40 minutes (see time line in Fig. 2; Foe, 1989), embryos stained for cyclin are more appropriate for following these divisions collectively.

Fig. 8 shows wild-type and embryos mutant for *tld*, *scw* and *dpp*, stained for cyclin A at stages prior to, and during division in δN. The panel at left shows gastrulating embryos at stage 8 in which unstained cells along the DV axis have just divided as part of δ11, and therefore do not contain any cyclin. In wild-type embryos, the mid-dorsal region corresponds to δA, which does not divide after cycle 13 and therefore still contains accumulated cyclin (Fig. 8A). No cells corresponding to δA can be seen in ventralizing mutants; cells in the mid-dorsal region of *tld* and *scw* embryos divide as part of δ11 (Fig. 8B,C). In older embryos at stage 9, cells lateral to δ11 are dividing as part of δN (Fig. 8E-G). The speckled appearence of these embryos is a result of ongoing mitoses in the region, which are late mitoses in δN. In *tld* and *scw* null mutants, an estimated 30-40% reduction occurs in the total number of cells contributing to δ11 (a moderately strong allele of *tld* is shown in Fig. 8B). This reduction in the size of dorsal domains can be correlated with an expansion of δN (Fig. 8E-G). In late stage embryos, cells that are close to the ventral midline still contain cyclin and are part of δM which divides last.

In *dpp* null mutants, which show the strongest ventralized cuticle, the shift in dorsal and dorsolateral domains is greater than in *tld* and *scw* embryos. As mentioned earlier, anteriorly both δ1 and δ5 meet across the dorsal midline. Posterior to the cephalic furrow, none of the dorsal cells divide as part of δ11 (compare embryos in Fig. 8A,D). This reduction in the size of δ11 again appears to correlate with an increase in size of δN. All cells along the DV axis (excluding δ14 and those that invaginate as part of the mesoderm), divide as part of δN and δM, constituting the ventral neuroectoderm (Fig. 8H). Such embryos show complete elimination of δA, δ19 and δ11, from dorsal and lateral positions along the axis (schematized in Fig. 9).

Despite the dorsal extension of δN, the size of domains δ16 and δ17 do not change in any of the ventralizing mutants (δ16 marked in Fig. 8B-D, position relative to the ventral midline marked with an asterisk in Fig. 9). δ16 and δ17 are paired clusters of cells, which are reiterated in each abdominal segment at a fixed position along the DV axis (Figs 2 and 8; Foe, 1989). Since δ16 and δ17 can be assumed to represent a subset of δN, the size of these domains should reflect the overall increase in the size of δN in the ventralized *tld*, *scw* and *dpp* mutants. The observation that the expansion of δN does not affect either the size or the position of δ16 and δ17 is important because it suggests that only a relatively dorsal part of the δN domain may have extended to compensate for the deletion of dorsal pattern elements.

In all of the ventralizing mutants, domains on the ventral side including δ4, δ8, δ10, δ14, δ15 and δ23, which correspond to the anterior and posterior midgut anlagen and the stomodeum, appear normal. We have confirmed that the number of cells expressing *sna* and *sim* is the same as in normal embryos (Ray et al., 1991; unpublished data).

In summary, the fate map changes in null mutants of the dpp group indicate a progressive loss of dorsally occurring domains δA, δ19 and δ11, in that order, along with the coordinated expansion of lateral and ventrolateral domains.

Allelic series of the dpp group genes suggest a graded function

Mutants at each individual locus of the dpp group can be ordered into a phenotypic series comprising partial

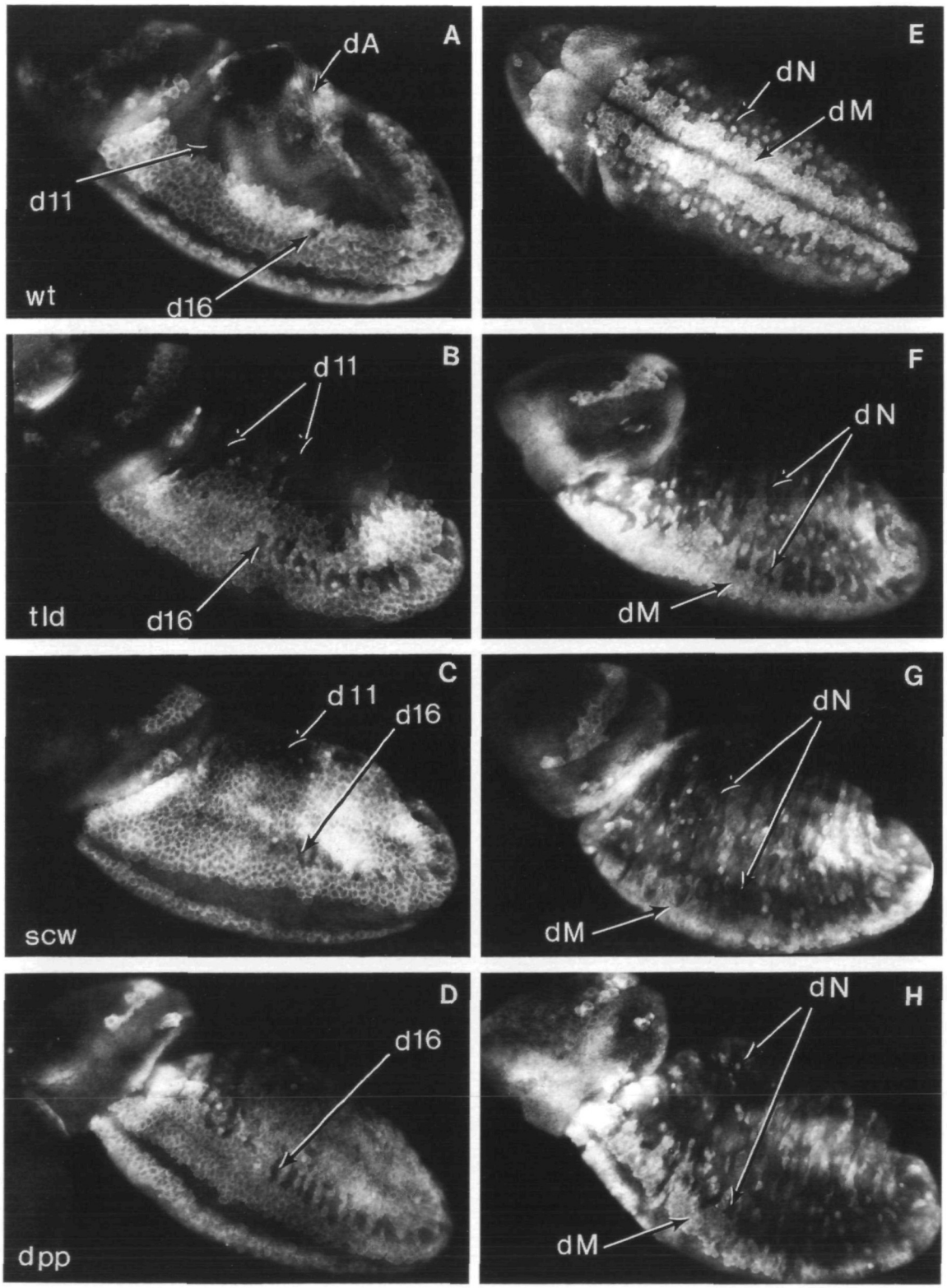

to complete loss-of-function alleles, the alleles in *trans*-heterozygous combinations and *in trans* to a deficiency for the locus (Table 1 and data not shown). The alleles listed in Table 1 are in increasing order of phenotypic strength (class I to V; characteristics used in classification are presented in the Materials and methods section).

The phenotypic classification of the *tld* alleles shown in Table 1 is based on the strength of ventralization exhibited by each mutant allele in the homozygous

Fig. 8. Fate map shift in mutants affecting dorsal pattern. Wild-type (A, E) and mutant embryos, tld^{9B} (B, F), scw^{S12} (C, G), dpp^{Hin46} (D, H), are shown stained for cyclin A to illustrate the shift in position of ventrolateral domains. Embryos are oriented with anterior at top left corner and the lateral side showing, except for the embryo in (E) which is viewed ventrally. Embryos in panel at left are at stage 8, and in the panel at right at stage 9. In the wild-type embryos (A), dorsalmost cells in δA, which do not divide in cycle 14, show accumulated cyclin, but dorsolateral cells in δ11 have divided and thus do not stain for cyclin. In *tld* and *scw* mutants (B, C), δA is missing replaced by the dorsally shifted δ11. At the same stage in a *dpp* mutant (D), both δA and δ11 are missing. Cells in δ16 and δ17, which normally follow division in δ11 by 10 minutes, are seen in the embryos at left (A-D, δ16 is marked; δ16 and δ17 alternate along the anterior-posterior axis). In stage 9 embryos (E-F), the ventrolateral cells (δN) have embarked on metasynchronous divisions characteristic of this region, therefore exhibiting a speckled appearence. In the wild-type embryo (ventral view in E), δN divisions are restricted to a strip of cells on the ventrolateral surface. In the *tld* and *scw* mutants (lateral views in F, G), δN divisions extend to more dorsal positions (arrows mark the width of the region in one half of the embryo). In the *dpp* mutant (H), all cells including the dorsal most cells are seen dividing at this time. The width of δM appears unaltered.

condition. In addition, alleles at this locus show a complex complementation behaviour (G. Jürgens, personal communication; this study), which affects their placement in this series. With the exception of tld^{10E}, tld^{6P4} and tld^{9Q1}, all alleles of *tld* show a small percentage of escapers (4%-23% of expected, see Materials and methods) in specific allelic combinations and *in trans* to a deficiency for the gene. In combination with the weak alleles tld^{5H} and tld^{7M}, an even greater percentage (25-38%) of the *trans*-heterozygous *tld* embryos survive to adulthood. Conversely, with the alleles tld^{10E}, tld^{6P4} or tld^{9Q1}, < 2% escapers are encountered in *trans*-allelic combinations and there is a consistently more severe phenotypic effect than *in trans* to a deficiency for *tld*. These latter three alleles represent antimorphic mutations in the *tld* gene (Ferguson and Anderson, in press).

In the allelic series of ventralizing genes, shown in Table 1, a graded loss of first dorsal and then lateral cuticular structures is encountered, which is correlated with an expansion of ventral pattern elements (see *dpp* alleles of different phenotypic strengths in Fig. 1D, G,J). Alleles exhibiting the same strength of ventralization can be encountered among mutations in the different dpp group genes (Fig. 1D-I and Table 1). Thus, the partial loss-of-function alleles of genes with strong null phenotypes like *tld*, *scw* and *dpp*, result in a weak ventralized phenotype remarkably like that of null alleles of *zen* and *srw* (Table 1).

Within an allelic series of each of the dpp group genes, dorsally placed mitotic domains, both in the cephalic and the middle body region, disappear in the same order as in the weak to strongly ventralized null mutants described above (data not shown). Irrespective of the genotype, there is a strict correlation between the order in which dorsally placed mitotic domains are truncated/lost and the phenotypic strength of the mutant allele. This observation strongly suggests that the function of the ventralizing genes has a graded effect on pattern formation in the dorsal half of the embryo.

Double mutant phenotypes of mutations in genes required for the specification of dorsoventral pattern

Mutations in the five ventralizing genes *zen*, *srw*, *tld*, *scw* and *dpp*, result in qualitatively similar effects, but each gene is unique in the extent to which it affects the dorsal pattern. In order to examine the possibility that the strength of the mutant phenotypes reflects a hierarchy of gene regulation, or alternatively that these genes provide independent inputs into the system, we examined the double mutant phenotypes. The phenotypes of the double mutants were characterized on the basis of their cuticular defects, such as deletions in the head skeleton, the increased width of ventral setal belts and the morphology/amount of Filzkörper material in the spiracles.

Null mutations in *zen* do not enhance the phenotype of null mutants of other dpp group genes. This is consistent with the molecular data regarding the lack of maintenance of *zen* expression in other mutants of the dpp group genes (Ray et al., 1991, see discussion). These data strongly support the idea that *zen* acts downstream of the other ventralizing genes.

In double mutant combinations between the remaining dpp group genes, two alleles exhibiting the same phenotypic strength show a stronger effect in combination, i.e. a larger region is affected than in either single mutant. Representative class I alleles of *zen*, *srw*, *scw*, *tld* and *dpp*, as well as class II and class III alleles of *scw*, *tld* and *dpp* were tested (see Materials and methods for exact genotypes). This observation suggests that these genes fulfill at least partly independent functions and do not fall into a simple regulatory hierarchy. In combinations between null mutants of the above genes, embryos homozygous mutant for one gene reveal a dosage sensitivity for the loss of the other. For example, srw^{B18} homozygous mutant embryos in combination with scw^{S12} heterozygous mutants show a phenotype comparable with class III ventralizing alleles. The double null mutant *scw; srw* however, is only marginally stronger than the *scw* null phenotype. This dosage sensitivity was observed in *srw, tld* and in *scw; tld* double nulls as well. Significantly, in none of the combinations is the degree of ventralization as strong as that of the null *dpp* allele.

The *dpp* null phenotype is not enhanced in combination with mutations in any other gene belonging to the group. This epistasis of the *dpp* phenotype over each of the ventralizing mutants reinforces the notion that this gene plays a key role in the specification of dorsal pattern.

Double mutants between mutations affecting dorsal pattern (the dpp group) and those that affect the ventral

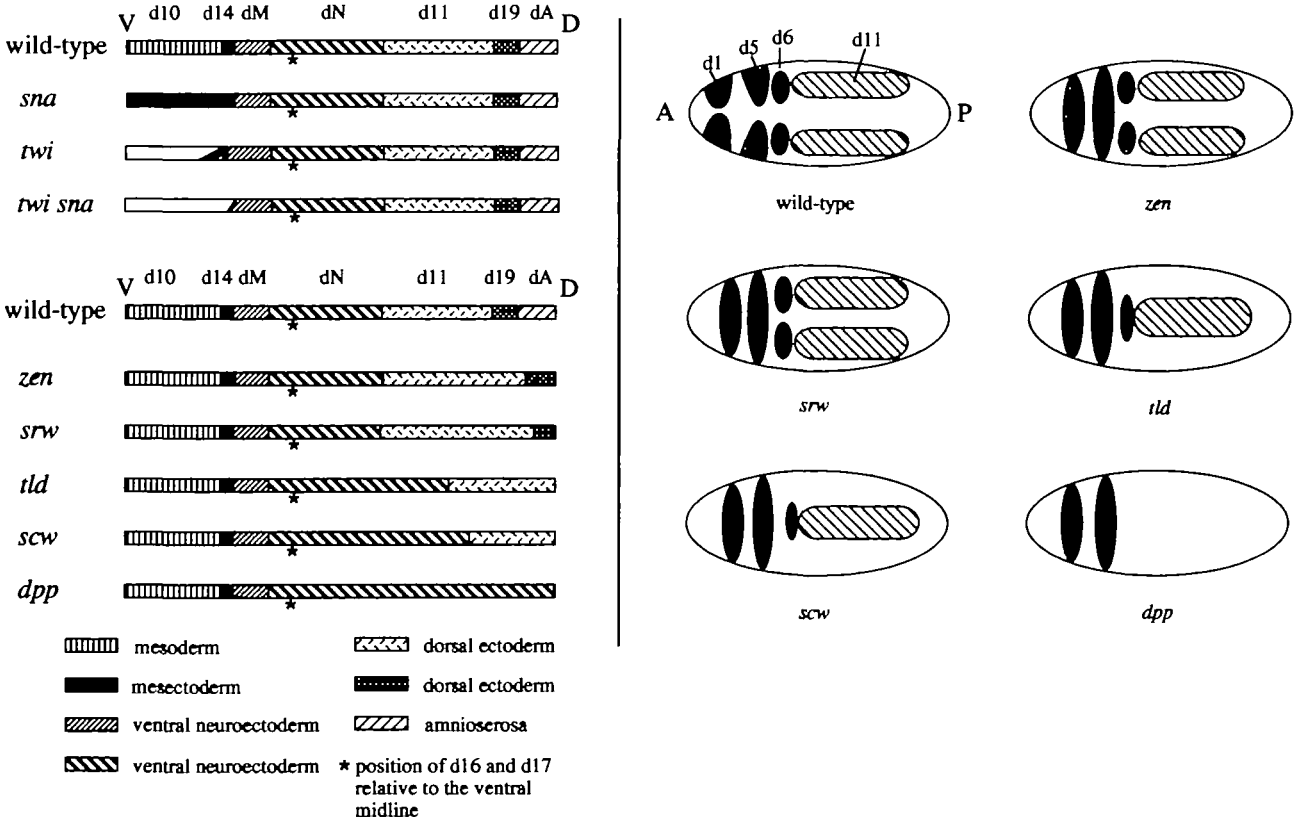

Fig. 9. Summary of the fate map changes in mitotic domains in dorsoventral pattern mutants. At left, the maps show the domains that occur in the middle body region along the entire axis, extending from the ventral midline (V) to the dorsal midline (D). The correlation of domains with their normal fates is shown (based on Foe, 1989). The maps refer to the altered domains in mutant alleles which represent null or strong loss-of-function mutants at each locus, *i.e.* *Df(2R)twiS60*, sna^{I1G}, zen^{w36}, srw^{B18}, tld^{B4}, scw^{S12} and dpp^{Hin46}. In *twi* mutants, the position of δ14 is shifted ventrally, but the remaining ventral cells do not divide. In *sna* mutants, the mesectoderm extends into the region which normally forms the mesodermal analagen in wild-type embryos. In *twi sna* double mutants, both mesoderm and the mesectoderm are missing and ventral cells behave uncharacteristically. The boundary between these cells and those in δM is not well defined. In the ventralizing mutants *zen* and *srw*, lateral domains δ19 and δ11 are shifted dorsally accompanied by the graded loss of dorsal pattern elements. In the stronger ventralizing mutants *tld*, *scw* and *dpp*, there is an extension of the dorsal boundary of δN as well. In the right-hand panel, the relative position of select mitotic domains on the surface of the dorsal blastoderm have been depicted schematically. Domains in each embryo are as marked for the wild-type. Anterior (A) and posterior (P) mark orientation of embryos. The dorsal boundaries of δ1 and δ5 are closer together relative to that of δ6, explaining why δ1 and δ5 are the first to show the dorsal shift of position values in weak ventralizing mutants *zen* and *srw*; followed by the shift in position of δ6 in *tld* and *scw*. In wild-type, the ventral boundary of δ6 is at a more dorsal position than that of δ1 and δ5. δ6 is the first to be eliminated in the strongest ventralized mutant, *dpp*.

side (*twi* and *sna*), show an additive effect on pattern. The double mutant larvae show deletion phenotypes characteristic of both sets of mutations but do not seem to cause stronger defects, implying that the two sets of information provided by these groups of genes act independently of each other.

Discussion

Fate mapping using mitotic division patterns

The mitotic pattern of the embryo reveals that there are fine partitions along the DV axis and allows the delineation of boundaries between cells with different tissue fates. We find a clear correlation between the early changes observed in the mitotic behaviour of mutant embryonic cells and the later cuticular phenotype of the mutants. We have demonstrated that the fate map shifts identified using the domains of division can be correlated with the altered expression of molecular markers such as the *sim* gene. These results emphasize the possibility of deriving fate maps of mutants with a similar precision to those obtained for mutants affecting the anterior-posterior axis by studying the alteration in segmentally repeated expression of pair-rule genes (Carroll et al., 1986; Frohnhöeffer and Nusslein-Volhard, 1987).

There is precedent for using mitotic domains as markers of cell fate. In embryos derived from *dl* mutant mothers, all cells along the DV circumference divide in concert as part of mitotic domains characteristic of the dorsal cells in a normal embryo (Foe and Odell, 1989).

Embryos derived from mothers that contain multiple copies of the *bicoid* (*bcd*) gene show an expansion and posterior shift in the boundaries of specific mitotic domains in the head region (Foe and Odell, 1989). Fate map shifts in these embryos (which have an enlarged cephalic region) have been demonstrated using the altered pattern of *eve* stripes (Driever and Nusslein-Volhard, 1988).

The link between the altered developmental pathway and the altered mitotic patterns in mutants remains to be critically examined. Our study shows that in some cases, for example in the *twi* mutants, mitotic activity specific to certain cell types is eliminated in the absence of genes that are required to specify particular cell fates. This observation suggests that some step that triggers the entry of cells into mitosis is also regulated by genes involved in specifying positional information. The three cell cycles following cellularization are dependent on zygotic transcription, in particular of the *string* (*stg*) gene product (Edgar et al., 1986; Edgar and O'Farrell, 1990). *stg* expression corresponds perfectly with the mitotic domains mapped by Foe (1989), but precedes the onset of mitosis in a given domain by ~20 minutes (Edgar and O'Farrell, 1989). In *dl* and *bicoid* mutant embryos, *stg* expression pattern is altered in a manner comparable with the altered mitotic domains reported by Foe and Odell (1989; B. Edgar, personal communication). Consistent with our results, δ10 (mesoderm) specific expression of *stg* is deleted in *twi* mutants. These data provide support for the correlation made in our study between cell fate and the timing of mitosis in embryonic cells. Further, they suggest that genes involved in pattern-formation, either directly or indirectly, regulate domain specific expression of the *stg* gene.

Role of the twi *and* sna *genes in establishing the mesoderm and the mesectoderm*

The fate mapping data show that the development of large regions of the embryo along the DV axis are under the control of two sets of zygotic genes, one set required on the dorsal side and the other on the ventral side. Several lines of evidence indicate that pattern formation in the two regions is established independently. Double mutants belonging to the two classes of genes show an additive effect on larval pattern. The expression patterns of the cloned genes belonging to the two groups do not overlap (except at the poles) and are not cross regulated (Ray et al., 1991).

On the ventral side, the absence of mitotic divisions specific to the mesoderm in both *twi* and *sna* mutants, indicates a requirement for both gene products in the establishment of the prospective mesoderm. However, the effect of the two mutations on the fate of ventral cells is qualitatively different (see schematic representation of fate map changes in Fig. 9, left panel). Mutations in *sna* affect cell fates in the prospective mesodermal anlagen alone. This is consistent with *sna* expression at cellular blastoderm, which is confined to the cells that invaginate and form the mesoderm (Leptin and Grunewald, 1990; Ray et al., 1991). In *sna* mutants, these ventral cells switch to a behaviour normally encountered in the mesectodermal cells that form a boundary between the mesoderm and the ventral neuroectoderm, suggesting that one of the functions of *sna* is to repress mesectodermal fates in the prospective mesodermal cells. This function of *sna* is supported by the ectopic expression of the *sim* gene in *sna* mutants (Fig. 4F; Nambu et al., 1990; Leptin and Grunewald, 1990). *sna* also represses *rhomboid* and T3 (a member of the achaete-scute complex), which are normally expressed in the neuroectoderm and excluded from the mesoderm (Kosman et al., 1991).

In contrast, the absence of *twi* function does not result in a simple switch to an alternative fate, but rather to a ventral shift in the position of the mesectodermal anlagen. Several lines of evidence indicate that *twi* may act as a positive regulator of genes expressed in the mesoderm. Although *sna* expression is initiated independently of *twi* function, *sna* transcripts are expressed in a narrower region than normal in *twi* mutants, suggesting that the proper ontogeny of *sna* expression requires *twi* function (Ray et al., 1991; Kosman et al., 1991). Our results suggest that *twi* may also have a weak positive effect on the expression of *sim*, since its expression is delayed in *twi* mutants. *twi* protein is weakly expressed in 4-5 cells beyond the lateral boundaries of the cells expressing *sna* (Kosman et al., 1991), making it plausible that the two genes could set up a domain of *sim* expression, *twi* helping to establish the lateral extent and *sna* the ventral boundary. The partial and irregular ventral shift of the mesectodermal domain seen in *twi* embryos can be explained by the premature loss of *sna* expression.

We have shown that, even though *sim* is expressed in *twi* and *sna* mutant embryos the *sim* transcript is absent from *twi sna* double mutants (Fig. 5B). This result implies that the concerted activity of both genes is required for the proper establishment of the mesectoderm in addition to their requirement in the mesoderm. In the double mutant, the ventral cells that would have formed these tissues appear not to be specified, in that they do not behave like cells in another mitotic domain or divide at any time during cycle 14. Cells in the mesectodermal domain contribute to the formation of the ventral nervous system (Crews et al., 1988; Thomas et al., 1988; Nambu et al., 1990). In *sim* mutants, there is a loss of specific glial cells in the ventral nerve cord as well as a part of the ventral ectoderm (Crews et al., 1988; Thomas et al., 1988; Mayer and Nüsslein-Volhard, 1988). This may be relevant to the fact that there is a more severe cuticular phenotype of the double mutant compared to *twi* mutants alone, which retain the mesectodermal anlagen.

Specification of the dorsal pattern by dpp group genes

In contrast to genes affecting ventral pattern, mutations in the dpp group genes all affect dorsal pattern in a qualitatively similar manner, although with varying severity. The phenotype of the mutant embryos indicates that a reduction of activity in any of these genes results in a loss of dorsal structures accompanied

by an expansion of pattern elements derived from more lateral or ventrolateral anlagen.

The strongest fate map shifts are seen in the mutants *tld*, *scw* and *dpp*, which show an expansion of the ventrolateral neuroectoderm (δN) at the cost of dorsally occurring pattern elements, accounting for the progressive deletion of dorsal epidermis in these mutants. Interestingly, all pattern elements of the domain δN (as assessed by the position of δ16 and δ17) do not expand in a linear manner, although the boundary between the neuroectoderm (δN) and the dorsal epidermis (δ11) is shifted progressively to more dorsal positions in *tld*, *scw* and *dpp* mutants (Fig. 9). Since δ16 and δ17 are part of δN, any change in size of δN can be expected to be reflected in the size and position of δ16 and δ17. The implication of this result is that there may be a transformation of dorsal cells to a subset of δN, which is not delineated as a unique mitoitc domain. Supporting this idea, molecular markers (such as the late de novo expression of *dpp*), normally expressed in a narrow lateral stripe along the anterior-posterior axis, are expressed as a broad stripe encompassing the dorsal half of the embryo in *tld*, *scw* and *dpp* mutants (R. Ray and K. Arora, unpublished data).

The fate map shifts observed in the ventralizing mutants extend beyond the middle body region. There is a dorsal shift in the position of the cephalic furrow, apparent early during gastrulation. The shifts in the position of the dorsally placed mitotic domains (schematized in Fig. 9) can be correlated with the loss of cephalic structures like the optic lobes in *zen* mutants (Wakimoto et al., 1984) and with the defective head skeleton in the strongly ventralized *scw*, *tld* and *dpp* mutants (this work), since cells constituting δ1, δ5 and δ6 secrete the specialized cuticle of the mouthparts and generate the head sensory organs (fate map in Fig. 2; Jürgens et al., 1986). These observations reinforce the notion that, in ventralizing mutants, successive boundaries between dorsal and dorsolateral positions are first shifted in a more dorsal direction and subsequently eliminated in stronger mutants.

The allelic series of the mutant cuticular phenotypes and the fate map analysis support the idea that the weak-to-strong ventralized phenotypes are caused as a result of graded shifts in position information along the DV axis. It appears that the dorsal cells are sensitive to some product in their local environment, so that high and intermediate levels are correlated with dorsal and dorsolateral development, while the absence of the factor channels all cells into a ventrolateral pathway of development. The fact that *zen* and *dpp* expression is initiated in a common subset of dorsal cells (Rushlow et al., 1987b; St. Johnston and Gelbart, 1987), suggests that the positional information specified by *dl* is not sufficient to provide the complexity observed in the final embryonic pattern.

A plausible candidate for such a graded factor is the *dpp* gene product. Weak *dpp* alleles lack only the amnioserosa and, in moderately strong to null alleles, larger regions of the dorsal epidermis are deleted in addition to the amnioserosa. In the absence of the *dpp* gene product, all cells in the dorsal half of the embryo behave as ventral epidermal cells (Irish and Gelbart, 1987; our results). The fact that *dpp* null alleles exhibit a haplo-insufficiency suggests strongly that dorsal cells are very sensitive to a reduction in the *dpp* product. These data have resulted in the suggestion that *dpp* activity is in the form of a gradient with its highest level at the dorsal midline (Irish and Gelbart, 1987; K. Wharton and R. Ray, personal communication; Ferguson and Anderson, in press). The protein encoded by *dpp* shares homology to a family of TGF-β growth factors, some members of which are known to be secreted (Padgett et al., 1987). Recently, Panganiban et al. (1990) have demonstrated that the *dpp* protein is secreted in *Drosophila* tissue culture cells and subsequently processed.

dpp expression is unaltered in any of the ventralising zygotic mutants (Ray et al., 1991). These results place the *dpp* gene early in the hierarchy of events regulating dorsal development, or alternatively, assign it a role in which it acts independently of the ventralizing genes. A third possibility is that some of the genes that control dorsal specification, do so by regulating *dpp* activity rather than its distribution. Since *dpp* transcripts appear to be uniformly expressed in the dorsal blastoderm (St. Johnston and Gelbart, 1987), any gradient of *dpp* activity most probably occurs at the post-transcriptional level. Consistent with this hypothesis, the recently cloned *tld* product, which shares homology with the human bone morphogenetic protein, BMP1, contains an N-terminal metalloprotease domain (Shimell et al., 1991). BMP1 was identified by virtue of its property of co-purifying with BMP2, a mammalian homolog of *dpp*, and another member of the TGF-β family (Wozney et al., 1988). This makes it highly plausible that *tld* is involved in post-translational activation of *dpp* or regulates its interaction with a receptor.

Our analysis of the double mutant phenotypes of mutations in the dpp group genes, places *zen* downstream of the remaining genes. Although the initial expression of *zen* is dependent only on maternal effect genes, in the absence of the other dpp group genes *zen* expression is rapidly lost and does not refine into the discrete band of expression coincident with cells forming the amnioserosa (Rushlow and Levine, 1990; Ray et al., 1991). The fact that *zen* encodes a homeodomain containing protein and could be involved in regulating the transcription of other genes involved in differentiation, is consistent with its suggested function of specifying the amnioserosa (Rushlow et al., 1987b; Doyle et al., 1989).

Since *dpp* appears to be the primary gene involved in specifying dorsal fates, the simplest explanation of the ventralized phenotypes would be the suppression by *dpp* of some gene activities(s) that are responsible for the formation of the ventral neurogenic ectoderm and may be sensitive to levels of *dpp* activity as well. The TGF-β family of secreted polypeptides mediates intercellular communication in a multitude of organisms and appears to control a wide range of biological processes including cell growth and differentiation (Massagué,

1990). Like *dpp*, many members of the family appear to be important morphogenesis factors. Recent experiments have shown that activin-related polypeptides (another TGF-β family member), can play instructive roles in the axial patterning of *Xenopus* and chicken embryos (Smith et al., 1990). *In situ* hybridization experiments with developing mouse embryos have shown that BMP2 and BMP4 are expressed in a wide variety of tissues (Jones et al., 1991), suggesting that in addition to inducing de novo bone growth, they may play more general roles in patterning the mammalian embryo. In a similar fashion, it is possible that *dpp* initiates a signal transduction pathway that results in the transcriptional activation of downstream genes responsible for the differentiation of dorsal pattern.

We thank V. Foe for providing the initial guidance in studying the mitotic domains and for sharing unpublished data, S. Roth, G. Jürgens, R. Lehmann and H. Frohnhöfer for several stimulating discussions and R. Warrior, D. Stein, R. Ray and C. Rushlow for valuable comments on the manuscript. R. Grömke-Lutz helped in producing the figures. K. Arora was supported by a Fellowship from the Max Planck Society.

References

Anderson, K. V. (1987). Dorsal-ventral embryonic pattern genes of *Drosophila*. *Trends Genet.* **3**, 91-97.

Anderson, K. V., Bokla, L. and Nüsslein-Volhard, C. (1985b). Establishment of dorsal-ventral polarity in the *Drosophila* embryo: The induction of polarity by the *Toll* gene product. *Cell* **42**, 791-798.

Anderson, K. V., Jürgens, G. and Nüsslein-Volhard, C. (1985a). Establishment of dorsal-ventral polarity in the *Drosophila* embryo: genetic studies on the role of the *Toll* gene product. *Cell* **42**, 779-789.

Anderson, K. V. and Nüsslein-Volhard, C. (1986). Dorsal-group genes of *Drosophila*. In *Gametogenesis and the Early Embryo*. (ed. J. Gall) pp. 177-194. New York: Alan R. Liss. Inc.

Boulay, J. L., Dennefeld, C. and Alberga, A. (1987). The *Drosophila* developmental gene *snail* encodes a protein with nucleic acid binding fingers. *Nature* **330**, 395-398.

Busson, D., Gans, M., Komitopoulou, K. and Mason, M. (1983). Genetic analysis of three dominant female-sterile mutations located on the X-chromosome of *Drosophila melanogaster*. *Genetics* **105**, 309-325.

Campos-Ortega, J. A. and Hartenstein, V. (1985). *The Embryonic Development of* Drosophila melanogaster. Berlin: Springer-Verlag.

Carroll, S. B., Winslow, G. M., Schüpbach, T. and Scott, M. P. (1986). Maternal control of *Drosophila* segmentation gene expression. *Nature* **323**, 278-280.

Crews, S. T., Thomas, J. B. and Goodman, C. S. (1988). The *Drosophila single-minded* gene encodes a nuclear protein with a sequence similarity to the *per* gene product. *Cell* **52**, 143-151.

Doyle, H. J., Harding, K., Hoey, T. and Levine, M. (1986). Transcripts encoded by a homeobox gene are restricted to dorsal tissues of *Drosophila* embryos. *Nature* **323**, 76-79.

Driever, W. and Nüsslein-Volhard, C. (1988). The *bicoid* protein determines position in the *Drosophila* embryo in a concentration dependent manner. *Cell* **54**, 95-104.

Edgar, B. A., Keihle, C. P. and Schubiger, G. (1986). Cell cycle control by the nucleo-cytoplasmic ratio in early *Drosophila* development. *Cell* **44**, 365-372.

Edgar, B. A. and O'Farrell, P. H. (1989). Genetic control of cell division patterns in the *Drosophila* embryo. *Cell* **57**, 177-187.

Edgar, B. A. and O'Farrell, P. H. (1990). The three postblastoderm cell cycles of *Drosophila* embryogenesis are regulated in G2 by *string*. *Cell* **62**, 469-480.

Ferguson, E. L. and Anderson, K. V. (1992). Localized enhancement and repression of the activity of the TGF-β family member, *decapentaplegic*, is necessary for dorsal-ventral pattern formation in the *Drosophila* embryo. *Development* (in press).

Foe, V. E. (1989). Mitotic domains reveal early commitment of cells in *Drosophila* embryos. *Development* **107**, 1-25.

Foe, V. E. and Alberts, B. M. (1983). Studies of nuclear and cytoplasmic behaviour during the five mitotic cycles that precede gastrulation in *Drosophila* embryogenesis. *J. Cell Sci.* **61**, 31-70.

Foe, V. E. and Odell, G. M. (1989). Mitotic domains partition fly embryos, reflecting early cell biological consequences of determination in progress. *Am. J. Zool.* **29**, 617.

Frohnhöfer, H. G. (1982). Der Einfluß von Maternalem und Zygotischem Genom auf die Musterbildung in *Drosophila melanogaster*. Diploma Thesis. Tübingen, FRG.

Frohnhöfer, H. G. and Nüsslein-Volhard, C. (1986). Maternal genes required in the anterior localization of *bicoid* activity in the embryo of *Drosophila*. *Genes Dev.* **1**, 880-890.

Ghosh, S., Gifford, A. M., Riviere, L. R., Tempst, P., Nolan, G. P. and Baltimore, D. (1990). Cloning of the p50 DNA binding subunit of NF-κB: homology to *rel* and *dorsal*. *Cell* **62**, 1019-1029.

Grau, Y., Cateret, C. and Simpson, P. (1984). Mutations and chromosomal rearrangements affecting the expression of *snail*, a gene involved in embryonic patterning in *Drosophila melanogaster*. *Genetics* **108**, 347-360.

Hartenstein, V. and Campos-Ortega, J. A. (1985). Fate mapping in the wild-type *Drosophila melanogaster* 1. The spatio-temporal pattern of embryonic cell division. *Roux's Arch. Dev. Biol.* **194**, 181-195.

Ingham, P. W. (1988). The molecular genetics of embryonic pattern formation in *Drosophila*. *Nature* **335**, 25-33.

Ip, T., Kraut, R., Levine, M. and Rushlow, C. A. (1991). The *dorsal* morphogen is a sequence-specific DNA-binding protein that interacts with a long range repression element in *Drosophila*. *Cell* **64**, 439-446.

Irish, V. F. and Gelbart, W. M. (1987). The *decapentaplegic* gene is required for dorsal-ventral patterning of the *Drosophila* embryo. *Genes Dev.* **1**, 868-879.

Jones, M. C., Lyons, K. M. and Hogan, B. (1991). Involvement of Bone Morphogenetic Protein-4 (BMP-4) and Vgr-1 in morphogenesis and neurogenesis in the mouse. *Development* **111**, 531-542.

Jürgens, G. (1987). Segmental organisation of the tail region in the embryo of *Drosophila melanogaster*. A blastoderm fate map of the cuticule structures of the larval tail region. *Roux's Arch. Dev. Biol.* **196**, 141-157.

Jürgens, G., Lehmann, R., Schardin, M. and Nüsslein-Volhard, C. (1986). Segmental organisation of the head in the embryo of *Drosophila melanogaster*. A blastoderm fate map of the cuticle structures of the larval head. *Roux's Arch. Dev. Biol.* **195**, 359-377.

Jürgens, G., Wieschaus, E. and Kluding, H. (1984). Mutations affecting the pattern of the larval cuticle in *Drosophila melanogaster*. II. Zygotic loci on the third chromosome. *Wilhelm Roux's Arch. Dev. Biol.* **193**, 283-295.

Karr, T. L. and Alberts, B. M. (1986). Organisation of the cytoskeleton in early *Drosophila* embryos. *J. Cell Biol.* **102**, 1494-1509.

Kieran, M., Blank, V., Logeat, F., Vandekerckhove, J., Lottspeich, F., Le Bail, O., Urban, M. B., Kourilsky, P., Baeuerle, P. A. and Israël, A. (1990). The DNA binding subunit of NF-κB is identical to factor KBF1 and homologous to the *rel* oncogene product. *Cell* **62**, 1007-1018.

Klingler, M., Erdelyi, M., Szabad, J. and Nüsslein-Volhard, C. (1988). Function of *torso* in determining the terminal anlagen of the *Drosophila* embryo. *Nature* **335**, 275-277.

Kosman, D., Ip, T., Levine, M. and Arora, K. (1991). The establishment of the mesoderm-neuroectoderm boundary in the *Drosophila* embryo. *Science* **254**, 118-122.

Lehner, C. F. and O'Farrell, P. H. (1989). Expression and function of *Drosophila* cyclin A during embryonic cycle progression. *Cell* **56**, 957-968.

Lehner, C. F. and O'Farrell, P. H. (1990). The roles of *Drosophila* cyclins A and B in mitotic control. *Cell* **61**, 535-547.

Leiss, D., Minz, U., Gasch, A., Mertz, R. and Renkawitz-Pohl, R. (1988). β3 tubulin expression characterizes the differentiating

mesodermal germ layer during *Drosophila* embryogenesis. *Development* **104**, 525-531.

Leptin, M. and Grunewald, B. (1990). Cell shape changes during gastrulation in *Drosophila*. *Development* **110**, 73-84.

Lohs-Schardin, M., Cremer, C. and Nüsslein-Volhard, C. (1979). A fate map for the larval epidermis of *Drosophila melanogaster*: Localised cuticle defects following irradiation of the blastoderm with an ultraviolet laser microbeam. *Dev. Biol.* **73**, 239-255.

Massagué, J. (1990). The transforming growth factor-β family. *Annu. Rev. Cell Biol.* **6**, 597-641.

Mayer, U. and Nüsslein-Volhard, C. (1988). A group of genes required for pattern formation in the ventral ectoderm of the Drosophila embryo. *Genes Dev.* **2**, 1496-1511.

Murre, C., Schonleber McCaw, P. and Baltimore, D. (1989). A new DNA binding and dimerization motif in immunoglobin enhancer binding, *daughterless*, *MyoD* and *myc* binding proteins. *Cell* **56**, 777-783.

Nambu, J. R., Frank, R. G., Hu, S. and Crews, S. T. (1990). The *single-minded* gene of *Drosophila* is required for the expression of genes important for the development of CNS midline cells. *Cell* **63**, 63-75.

Nüsslein-Volhard, C. (1977). A rapid method for screening eggs from single *Drosophila* females. *Dros. Info. Service* **52**, 166.

Nüsslein-Volhard, C. (1979). Maternal effect mutations that alter the spatial coordinates of the embryo of *Drosophila melanogaster*. In *Determinants of Spatial Organization*. Academic Press, (ed. S. Subtelny and I. R. Koenigsberg), pp. 185-211. New York.

Nüsslein-Volhard, C., Kluding, H. and Jürgens, G. (1985). Genes affecting the segmental subdivision of the *Drosophila* embryo. *Cold Spring Harbor Symp. Quant. Biol.* **50**, 145-154.

Nüsslein-Volhard, C. and Roth, S. (1989). Axis determination in insect embryogenesis. In *Cellular Basis of Morphogenesis. Ciba Foundation Symposium* **144**. pp. 37-55. New York: John Wiley and Sons.

Nüsslein-Volhard, C., Wieschaus, E. and Kluding, H. (1984). Mutations affecting the pattern of larval cuticle in *Drosophila melanogaster* I: Zygotic loci on the second chromosome. *Wilhelm Roux's Arch. Dev. Biol.* **193**, 267-282.

Padgett, R. W., St Johnston, R. D. and Gelbart, W. M. (1987). A transcript from a *Drosophila* pattern gene predicts a protein homologous to the transforming growth factor-β family. *Nature* **325**, 81-84.

Panganiban, G. F., Rashka, K. E., Neitzel, M. D. and Hoffmann, F. M. (1990). Biochemical characterization of the *Drosophila dpp* protein, a member of the transforming growth factor β family of growth factors. *Mol. Cell. Bio.* **10**, 2669-2677.

Perrimon, N. (1984). Clonal analysis of dominant female-sterile germline-dependent mutations in *Drosophila melanogaster*. *Genetics* **108**, 927-939.

Ray, R., Arora, K., Nüsslein-Volhard, C. and Gelbart, W. M. (1991). The control of cell fate along the dorsal-ventral axis of the *Drosophila* embryo. *Development* **113**, 35-54.

Roth, S., Hiromi, Y., Godt, D. and Nüsslein-Volhard, C. (1991). *cactus*, a maternal gene required for proper formation of the dorsoventral morphogen gradient in *Drosophila* embryos. *Development* **112**, 371-388.

Roth, S., Stein, D. and Nüsslein-Volhard, C. (1989). A gradient of nuclear localization of the *dorsal* protein determines dorso-ventral pattern in the *Drosophila* embryo. *Cell* **59**, 1189-1202.

Rushlow, C. and Arora, K. (1990). Dorsal-ventral polarity and pattern formation in *Drosophila*. *Seminars in Cell Biology* **1**, 137-149.

Rushlow, C., Doyle, H., Hoey, T. and Levine, M. (1987b). Molecular characterization of the *zerknüllt* region of the Antennapedia gene complex in *Drosophila*. *Genes Dev.* **1**, 1268-1279.

Rushlow, C., Frasch, M., Doyle, H. and Levine, M. (1987a). Maternal regulation of *zerknüllt*: a homeobox gene controlling differentiation of dorsal tissues in *Drosophila*. *Nature* **330**, 583-586.

Rushlow, C., Han, K., Manley, J. L. and Levine, M. (1989). The graded distribution of the *dorsal* morphogen is initiated by selective nuclear transport in *Drosophila*. *Cell* **59**, 1165-1177.

Rushlow, C. and Levine, M. (1990). The role of the *zerknüllt* gene in dorsal-ventral pattern formation in *Drosophila*. *Adv Genet.* **27**, 277-304.

Shimell, M. J., Ferguson, E. L., Childs, S. and O'Connor, M. B. (1991). The *Drosophila* dorsal-ventral patterning gene *tolloid* is homologous to human Bone Morphogenetic Protein - 1. *Cell* **67**, 469-481.

Simpson, P. (1983). Maternal-zygotic gene interactions during formation of the dorsoventral pattern in *Drosophila* embryos. *Genetics* **105**, 615-632.

Smith, J. C., Price, B. M. J., Van Nimmen, K. and Huylebroeck, D. (1990). Identification of a potent *Xenopus* mesodermal induction factor as a homologue of activin A. *Nature* **345**, 729-731.

Spencer, F. A., Hoffman, F. M. and Gelbart, W. M. (1982). *Decapentaplegic*: A gene complex affecting morphogenesis in *Drosophila melanogaster*. *Cell* **28**, 451-461.

Steward, R. (1987). *dorsal*, an embryonic polarity gene in *Drosophila*, is homologous to the vertebrate proto-oncogene, *c-rel*. *Science* **238**, 692-694.

Steward, R. (1989). Relocalization of the *dorsal* protein from the cytoplasm to the nucleus correlates with its function. *Cell* **59**, 1179-1188.

Steward, R., Zusman, S. B., Juang, L. H. and Schedl, P. (1988). The *dorsal* protein is distributed in a gradient in the early *Drosophila* embryos. *Cell* **55**, 487-495.

St Johnston, R. D. and Gelbart, W. M. (1987). *decapentaplegic* transcripts are localized along the dorsal-ventral axis of the *Drosophila* embryo. *EMBO J.* **6**. 2785-2791.

Tautz, D. and Pfeifle, C. (1989). A non-radioactive *in situ* hybridization method for the localization of specific RNAs in *Drosophila* embryos reveals translation control of the segmentation gene *hunchback*. *Chromosoma* **98**, 81-85.

Technau, G. M. and Campos-Ortega, J. A. (1986). Lineage analysis in embryos of *Drosophila melanogaster*: II. Commitment and proliferative capabilities of neural and epidermal cell progenitors. *Roux's Arch. Dev. Biol.* **195**, 445-454.

Thisse, B., Stoetzel, C., Gorostiza-Thisse, C. and Perrin-Schmitt, F. (1988). Sequence of the *twist* gene and nuclear localization of its protein in endomesodermal cells of early *Drosophila* embryos. *EMBO J.* **7**, 2175-2183.

Thisse, B., Stoetzel, C., Messal, M. and Perrin-Schmitt, F. (1987). Genes of the *Drosophila* maternal dorsal group control the specific expression of the zygotic gene *twist* in presumptive mesodermal cells. *Genes Dev.* **1**, 709-715.

Thisse, C., Perrin-Schmitt, F., Stoetzel, C. and Thisse, B. (1991). Sequence-specific transactivation of the *Drosophila twist* gene by the *dorsal* gene product. *Cell* **65**, 1191-1201.

Thomas, J. B., Crews, S. T. and Goodman, C. S. (1988). Molecular genetics of the *single-minded* locus: A gene involved in the development of the *Drosophila* nervous system. *Cell* **52**, 133-141.

Wakimoto, B. T., Turner, F. R. and Kaufman, T. C. (1984). Defects in embryogenesis in mutants associated with the Antennapedia gene complex of *Drosophila melanogaster*. *Dev. Biol.* **102**, 147-172.

Wieschaus, E. and Nüsslein-Volhard, C. (1986). Looking at embryos. In *Drosophila: A Practical Approach*, (ed. D. B. Roberts), pp. 199-227, Washington, D. C.: IRL Press.

Wozney, J. M., Rosen, V., Celeste, A. J., Mitsock, L. M., Whitters, M. J., Kriz, R. W., Hewick, R. M. and Wang, E. A. (1988). Novel regulators of bone formation: Molecular clones and activities. *Science* **242**, 1528-1534.

(Accepted 28 October 1991)